

Triaxial Characterization of Light and Dense Backfill to Determine Properties for use in Numerical Modeling

NWMO TR-2008-05

March 2008

J.A. Blatz¹, G. Siemens² and A. Man³

¹University of Manitoba

²Royal Military College of Canada

³Atomic Energy of Canada Limited

nwmo

NUCLEAR WASTE
MANAGEMENT
ORGANIZATION

SOCIÉTÉ DE GESTION
DES DÉCHETS
NUCLÉAIRES



Nuclear Waste Management Organization
22 St. Clair Avenue East, 6th Floor
Toronto, Ontario
M4T 2S3
Canada

Tel: 416-934-9814
Web: www.nwmo.ca

**Triaxial Characterization of Light and
Dense Backfill to Determine Properties for use in Numerical Modeling**

NWMO TR-2008-05

March 2008

J.A. Blatz¹, G. Siemens² and A. Man³

¹University of Manitoba

²Royal Military College of Canada

³Atomic Energy of Canada Limited

Disclaimer:

This report does not necessarily reflect the views or position of the Nuclear Waste Management Organization, its directors, officers, employees and agents (the "NWMO") and unless otherwise specifically stated, is made available to the public by the NWMO for information only. The contents of this report reflect the views of the author(s) who are solely responsible for the text and its conclusions as well as the accuracy of any data used in its creation. The NWMO does not make any warranty, express or implied, or assume any legal liability or responsibility for the accuracy, completeness, or usefulness of any information disclosed, or represent that the use of any information would not infringe privately owned rights. Any reference to a specific commercial product, process or service by trade name, trademark, manufacturer, or otherwise, does not constitute or imply its endorsement, recommendation, or preference by NWMO.

ABSTRACT

Title: Triaxial Characterization of Light and Dense Backfill to Determine Properties for use in Numerical Modeling
Report No.: NWMO TR-2008-05
Author(s): J.A. Blatz¹ G. Siemens² and A. Man³
Company: ¹University of Manitoba, ²Royal Military College of Canada
³Atomic Energy of Canada Limited
Date: March 2008

Abstract

This report presents the results of triaxial testing directed at characterization of mechanical properties of light and dense backfill materials that contain freshwater as the pore fluid. The results of the triaxial testing program provide the isotropic consolidation and stress-strain properties of light backfill (LBF) and dense backfill (DBF) materials under saturated conditions. These properties are required parameters for simulating the behaviour of these materials during numerical modeling activities.

In the in-room emplacement geometry for used nuclear fuel, light and dense backfill materials will be required as barrier materials that will surround spent fuel containers and will support them in the short term during construction and in the long term following repository closure. In the in-floor geometry for container emplacement the backfill materials will be used to fill the access tunnels immediately above the emplacement boreholes, preventing upwards swelling of the buffer materials that surround them. These barrier materials will also be expected to conduct heat away from the waste containers to the surrounding rock and limit contaminant transport by groundwater. As a result of these requirements, establishing the mechanical performance of LBF and DBF under varying moisture, temperature, chemical and pressure conditions are critical to understanding their intended performance in underground disposal concepts. The test results presented in this report is part of the process of characterizing the mechanical behaviour of LBF and DBF under saturated conditions with freshwater as the pore fluid.

The testing program includes standard triaxial testing at three confining pressures (400 kPa, 800 kPa and 1,200 kPa) to establish the consolidation characteristics of the backfill materials under isotropic loading and shear characteristics under shear loading. The tests were conducted under both drained and undrained conditions for both materials. The results allow interpretation of both strength and deformation or stiffness parameters (Bulk Modulus and Young's modulus) providing materials parameters for use in numerical models. The work also included development of laboratory preparation procedures and standards for testing these two materials.

The results of the testing program indicate that the Bulk Modulus for the LBF is 2.8 MPa and the average Young's Modulus for the material is 155.9 MPa. The critical state strength envelope for the LBF has a slope of $M = 0.47$, with a corresponding critical state friction angle of 13.5° . The strength of this material is similar to that of natural glacial lake clays.

The DBF material was found to be both stiffer and stronger than the LBF. The Bulk Modulus for the DBF is 10.7 MPa and the average Young's Modulus for the material is 261.7 MPa. The critical state strength envelope for the LBF has a slope of $M = 1.10$, with a corresponding critical state friction angle of 28° .

Additional testing (i.e. triaxial consolidation testing) is required to confirm the above Bulk Modulus values and subsequently determine a Poisson's Ratio for the materials. Greater confidence is given to the Young's Modulus values presented in this report.

As part of the on-going series of tests associated with this work the tests described in this report are being repeated using saline pore fluid. This is being done to provide comparative values for materials exposed to groundwater conditions that might be encountered under the geochemical conditions present in Ordovician sedimentary rocks.

TABLE OF CONTENTS

	<u>Page</u>
ABSTRACT	v
1. INTRODUCTION.....	1
2. MATERIALS	2
2.1 LIGHT BACKFILL (LBF)	2
2.2 DENSE BACKFILL (DBF)	3
3. EXPERIMENTAL WORK	3
3.1 LIGHT BACKFILL (LBF) TESTS (UNIVERSITY OF MANITOBA).....	3
3.1.1 LBF Testing Program.....	3
3.1.2 LBF Testing Procedure	3
3.1.3 LBF Test Results	4
3.1.3.1 LBF Preliminary Specimen Preparation	4
3.1.3.2 LBF Tests With Constant Volume Saturation.....	4
3.1.3.3 LBF Tests With Constant Mean Effective Stress Saturation	5
3.1.3.4 LBF Tests With Increasing Mean Effective Stress Saturation	5
3.1.3.5 LBF Tests With Direct Pressure Saturation	5
3.1.4 LBF Strength and Deformation Parameters	6
3.2 DENSE BACKFILL (DBF) TESTS (UNIVERSITY OF MANITOBA).....	7
3.2.1 DBF Test Program.....	7
3.2.2 DBF Test Procedure	7
3.2.3 DBF Test Results.....	8
3.2.4 DBF Strength and Deformation Parameters	8
4. STATUS OF TRIAXIAL TESTING OF LBF AND DBF WITH SALINE PORE FLUID	9
5. SUMMARY.....	10
REFERENCES	11

LIST OF TABLES

	<u>Page</u>
Table 1: Matrix of Triaxial Tests on LBF.....	13
Table 2: Matrix of Triaxial Tests on DBF.....	13
Table 3: LBF Strength and Deformation Parameters.....	13
Table 4: DBF Strength and Deformation Parameters.....	14

LIST OF FIGURES

	<u>Page</u>
Figure 1: LBF Specimen GS-LB02: Saturation Phase (sleeve not removed).....	15
Figure 2: LBF Specimen GS-LB03: Saturation Phase.....	16
Figure 3: LBF Specimen GS-LB05: Saturation Phase.....	17
Figure 4: LBF Specimen GS-LB05: 200 kPa, 400 kPa and 800 kPa Consolidation Phases.....	18
Figure 5: LBF Specimen GS-LB05: Deviator Stress (q) Versus Axial Strain (ϵ_a).....	19
Figure 6: LBF Specimen GS-LB05: Change in Pore Pressure (Δu) Versus Axial Strain (ϵ_a).....	20
Figure 7: LBF Specimen GS-LB05: Deviator Stress (q) Versus Mean Effective Stress (p').....	21
Figure 8: LBF Specimen GS-LB06: Saturation Phase.....	22
Figure 9: LBF Specimen GS-LB07: Saturation Phase.....	23
Figure 10: LBF Specimen GS-LB08: Saturation Phase.....	24
Figure 11: LBF Specimen GS-LB06: 400 kPa Consolidation Phase.....	25
Figure 12: LBF Specimen GS-LB06: Deviator Stress Versus Axial Strain.....	26
Figure 13: LBF Specimen GS-LB06: Change in Pore Pressure Versus Axial Strain.....	27
Figure 14: LBF Specimen GS-LB06: Deviator Stress Versus Mean Effective Stress.....	28
Figure 15: LBF Specimen GS-LB09: Saturation Phases.....	29
Figure 16: LBF Specimen GS-LB10: Saturation Phases.....	30
Figure 17: LBF Specimen GS-LB11: Saturation Phases.....	31
Figure 18: LBF Specimen GS-LB12: Saturation Phases.....	32
Figure 19: LBF Specimen GS-LB14: Saturation Phases.....	33
Figure 20: LBF Specimen GS-LB15: Saturation Phases.....	34
Figure 21: LBF Specimen JB-LB16: Saturation Phases.....	35
Figure 22: LBF Specimen JB-LB17: Saturation Phases.....	36
Figure 23: LBF Drained Shear Response: Deviator Stress Versus Axial Strain.....	37
Figure 24: LBF Drained Shear Response: Deviator Stress Versus Mean Effective Stress.....	38
Figure 25: LBF Undrained Shear Response: Deviator Stress Versus Axial Strain.....	39
Figure 26: LBF Undrained Shear Response: Deviator Stress Versus Mean Effective Stress.....	40
Figure 27: LBF Critical State Strength Envelope: Deviator Stress Versus Mean Effective Stress.....	41
Figure 28: LBF Specimen GS-LB11 Volume Change During Drained Shearing at 400 kPa: Specific Volume Versus Mean Effective Stress.....	42
Figure 29: LBF Specimen GS-LB14 Volume Change During Drained Shearing at 800 kPa: Specific Volume Versus Mean Effective Stress.....	43
Figure 30: LBF Specimen GS-LB12 Volume Change During Drained Shearing at 1,200 kPa: Specific Volume Versus Mean Effective Stress.....	44
Figure 31: LBF Specimen JB-LB16 Volume Change During Drained Shearing at 1,200 kPa: Specific Volume Versus Mean Effective Stress.....	45

Figure 32: Isotropic Consolidation Data from Drained Tests on LBF Used for the Determination of the Bulk Modulus. The upper plot (a) was established by combining the end-of-consolidation data from the tests shown. The lower plot (b) was established from a single specimen (GS-LB05).....	46
Figure 33: DBF Specimen GS-DBF13: Saturation Phases.....	47
Figure 34: DBF Specimen JB-DBF14: Saturation Phases.....	48
Figure 35: DBF Specimen GS-DBF15: Saturation Phases.....	49
Figure 36: DBF Specimen JB-DBF16: Saturation Phases.....	50
Figure 37: DBF Specimen GS-DBF17: Saturation Phases.....	51
Figure 38: DBF Specimen GS-DBF18: Saturation Phases.....	52
Figure 39: DBF Specimen GS-DBF19: Saturation Phases.....	53
Figure 40: DBF Specimen GS-DBF20: Saturation Phases.....	54
Figure 41: DBF Drained Shear Response: Deviator Stress Versus Axial Strain.....	55
Figure 42: DBF Drained Shear Response: Deviator Stress Versus Mean Effective Stress	56
Figure 43: DBF Undrained Shear Response: Deviator Stress Versus Axial Strain	57
Figure 44: DBF Undrained Shear Response: Deviator Stress Versus Mean Effective Stress ...	58
Figure 45: DBF Critical State Strength Envelope: Deviator Stress Versus Mean Effective Stress	59
Figure 46: DBF Specimen GS-DBF15 Volume Change During Drained Shearing at 400 kPa: Specific Volume Versus Mean Effective Stress	60
Figure 47: DBF Specimen GS-DBF18 Volume Change During Drained Shearing at 800 kPa: Specific Volume Versus Mean Effective Stress	61
Figure 48: DBF Specimen GS-DBF13 Volume Change During Drained Shearing at 1,200 kPa: Specific Volume Versus Mean Effective Stress	62
Figure 49: DBF Specimen GS-DBF12 Volume Change During Drained Shearing at 1,200 kPa: Specific Volume Versus Mean Effective Stress	63
Figure 50: Isotropic Consolidation Data from Drained Tests on DBF Used for the Determination of the Bulk Modulus	64
Figure 51: LBF Specimen LBF-1004: Saturation Phase (In progress).....	65
Figure 52: LBF Specimen LBF-1006: Saturation Phase (In progress).....	66

1. INTRODUCTION

In the course of developing concepts for deep geologic disposal of used nuclear fuel, a number of clay-based materials have been identified as potential components of a repository sealing system. These include highly compacted bentonite (HCB), bentonite-sand buffer (BSB), light backfill (LBF) and dense backfill (DBF) material (Russell and Simmons 2003; Maak and Simmons 2005). BSB¹, which consists of equal dry weight proportions of bentonite clay and graded sand (compacted to a dry density of 1.7 Mg/m³), was initially identified as the primary component of a repository sealing system (AECL 1994; Baumgartner 1996; Johnson et al. 1994). BSB was subjected to extensive characterization through triaxial testing. Triaxial testing has provided the strength and deformation parameters needed for design and analysis of performance of BSB based barriers through numerical modeling.

LBF and DBF were not initially examined to the same level of detail as the BSB, as they were located further away from the container in the originally examined in-floor emplacement geometry. Subsequent addition of the in-room emplacement geometry to the options for container placement has required that the LBF and DBF receive a more detailed evaluation. The DBF is a densely compacted, high-aggregate content material that is expected to be used to fill the majority of the tunnel and room excavations. The lower density, higher clay content LBF would be used to fill volumes where it is not possible to attain high compacted density or where special performance requirements exist.

Triaxial testing is required to define the strength envelope and deformation (stiffness) characteristics of the materials being considered for repository sealing systems. A minimum of three tests, conducted at three different pressures is required to define a strength envelope. This is typically achieved by conducting three isotropically consolidated undrained (CI \bar{U}) tests. In order to obtain reliable deformation parameters, drained triaxial (CID) tests are also required. Drained tests differ from the CI \bar{U} tests in that the drainage leads to the specimen are left open during shearing thus allowing volume change. The results of the drained tests can be combined with the CI \bar{U} tests in the construction of the strength envelope, providing further confidence in the data.

The parameters obtained from triaxial testing include those that define the slope of the strength envelope, such as the critical state, M parameter and the corresponding friction angle. The consolidation data and the shearing portion of the drained triaxial tests provide deformation parameters, such as the Bulk Modulus and Young's Modulus, respectively. These parameters are needed for stress-deformation modeling of the repository sealing systems to evaluate the performance of various designs. Knowledge of the properties of these materials is particularly important when considering the emplacement of the massive used fuel containers currently being considered for deep geologic disposal. Large, massive containers will require the installation of sealing materials that are able to support them without experiencing unacceptably large displacements.

This report documents the results of tests conducted by the University of Manitoba intended to characterize the LBF and DBF and provide baseline mechanical performance information for these materials. The work includes a triaxial testing program that examines the strength and deformation properties of LBF and DBF materials that contain freshwater as the pore fluid. Material preparation was defined by Atomic Energy of Canada Limited (AECL) using standard property specifications already established for the two materials. Specimens were then

¹ Note: the BSB described in AECL (1994) and Johnson et al. (1994) is referred to a Reference Buffer Material (RBM) in those documents.

saturated in the triaxial apparatus prior to shearing, under both drained and undrained conditions. The final results allow interpretation of both strength and deformation parameters to be used in numerical models.

The next step in the characterization the LBF and DBF material is to examine the influence of other variables, such as environmental factors, on the strength and deformation parameters. Of significant importance to NWMO's Adaptive Phased Management concept is the addition of sedimentary rocks as a potential host medium for a repository.

Deep sedimentary rock formations have been studied in southern Ontario (Mazurek, 2004). The geological environment in this area consists of a Paleozoic sequence of shales, overlying Ordovician limestone. Groundwater in the deep limestone is saline with total dissolved solids concentrations in excess of 200 g/L. High salinities indicate old, potentially stagnant groundwater, which is a good characteristic of a potential repository rock formation. The influence of saline pore fluid on the performance of sealing materials needs to be understood. High salinities are known to influence the hydraulic conductivity, strength, and compressibility of clay based materials through depression of the clay particles' diffuse double layer and so it is anticipated that it will also affect their mechanical behaviour.

An on-going triaxial testing program is advancing the understanding of the LBF and DBF materials under such conditions by repeating the testing program described in this report using saline water (250 g/L CaCl_2) as the pore fluid. This study, which is being conducted at the Royal Military College of Canada (RMC) in Kingston, ON in conjunction with the University of Manitoba, is aimed at simulating the pore fluid chemistry of Ordovician sedimentary bedrock. Work on the second phase began in 2007 and is expected to be completed in 2008. A summary of progress to date on testing under saline condition is provided at the end of this report.

2. MATERIALS

2.1 LIGHT BACKFILL (LBF)

Light backfill is one of the components of the engineered barriers system described by Russell and Simmons (2003) and Maak and Simmons (2005) as part of a current concept for deep underground repositories. Light backfill, as described by Russell and Simmons (2003), is composed of 50% bentonite and 50% sand and would be placed at a dry density of 1,240 kg/m³ and a water content of 15% for an initial saturation of approximately 33%. Preparation procedures for all light backfill specimens used in this testing program are as described below.

LBF specimens for triaxial testing were prepared at the University of Manitoba. Un-compacted LBF material was provided to the University of Manitoba from AECL, contained in buckets. Following 48 hours of drying at 100° C in an oven, the light backfill un-compacted sample was removed and sealed in a mixing bowl to allow thermal equilibration with the laboratory while preventing absorption of moisture from the atmosphere. The required oven-dried mass of soil was pre-calculated and sufficient material to make the specimens and conduct water content analysis was measured out and gently mixed with water that is misted onto the light backfill in a mixing bowl to ensure uniform water distribution. Once the desired quantity of water was added, the moistened soil was placed inside a sealed bag to prevent any subsequent changes in water content. Triaxial specimens of 50 mm diameter were then statically compacted in five 20 mm lifts in a cylindrical mold (resulting total specimen height of 100 mm). The remaining soil

was used for moisture content measurement. Following compaction, the specimens were installed in a standard triaxial cell and standard procedures for saturated triaxial testing were followed including saturation, consolidation and shearing phases.

2.2 DENSE BACKFILL (DBF)

Dense backfill is an engineered barrier material described by both Russell and Simmons (2003) and Maak and Simmons (2005) and is proposed for use in underground repositories to backfill portions of emplacement rooms and the majority of access tunnels. As summarized by Russell and Simmons (2003), dense backfill is currently defined as being composed of 5% bentonite, 25% glacial lake clay and 70% crushed granite aggregate. It is compacted to a dry density of 2.12 Mg/m^3 , with 8.5% water content to give an initial saturation of 80%.

Compacted specimens for triaxial testing were prepared by AECL following a procedure similar to that used to make the LBF specimens. The exception to the above procedure was that the specimens were statically compacted in five 50 mm lifts in a 102 mm diameter cylindrical mold (due to a larger grain size). The only triaxial specimen preparation performed by the University of Manitoba (U of M) was trimming specimens to the required size for the triaxial cell.

3. EXPERIMENTAL WORK

3.1 LIGHT BACKFILL (LBF) TESTS (UNIVERSITY OF MANITOBA)

3.1.1 LBF Testing Program

Table 1 summarizes the tests that have been conducted on LBF as part of this contract. The testing program included testing at three different isotropic consolidation pressures (400 kPa, 800 kPa and 1,200 kPa). Prior to testing these specimens, a series of initial specimens were tested to gain confidence in the preparation process.

3.1.2 LBF Testing Procedure

Testing consisted of standard saturated triaxial testing, generally following ASTM D 4767 – Consolidated Undrained Triaxial Compression Test for Cohesive Soils (1995). Procedures for saturating and consolidating light backfill specimens evolved as knowledge about light backfill behaviour was gained. As this is one of the first testing programs for this material, standard saturation and consolidation procedures were not available. Consequently, a number of trials were conducted to determine the most appropriate approach for detailed testing.

The first preparation procedure attempted included a constant volume saturation phase where a steel sleeve was installed within the cell to confine the LBF during water uptake. Interpretation of saturation was difficult with the steel sleeve that surrounded the specimen and once the sleeve was removed, specimens began absorbing more water and expanding.

The second procedure attempted was to saturate specimens at a mean effective stress of 50 kPa followed by consolidation steps to final mean effective stresses of either 400 kPa, 800 kPa or 1,200 kPa, following standard consolidation procedures. It was found that the time required for such a consolidation process was months and would not allow for the completion of the testing matrix in a timely manner.

The third preparation procedure attempted included a constant volume saturation phase where cell pressure was increased to keep the specimen from expanding excessively and absorbing water that would subsequently have to be expelled during consolidation. Consolidation phase durations were still excessive and therefore, the test process was modified.

The fourth preparation procedure, the one ultimately selected, was similar to the previously described constant volume procedure except that the final effective stress was applied at the initiation of the saturation phase. Once specimens were saturated, they were sheared. Testing following this procedure will provide information that is required to determine the strength and deformation parameters for characterization of light backfill. The Bulk Modulus, which is typically determined from increments in the consolidation phase using a single sample, can be determined by combining the results from separate specimens consolidated to different mean effective stress. This method allowed testing to proceed within a reasonable amount of time while still providing the required information.

Saturation of the specimens was determined by conducting B tests. A B test consists of applying an increase in cell pressure while the specimen drainage is closed. The subsequent increase in pore pressure is measured. The B value is determined by dividing the measured increase in pore pressure by the applied increase in cell pressure. Theoretically, a completely saturated specimen will display an increase in pore pressure that is equal to the applied increase in cell pressure for a B value of 1.0 (i.e. 100%). A minimum B value of 0.95 (i.e. 95%) was achieved prior to shearing, which is typical for commercial triaxial testing applications.

3.1.3 LBF Test Results

Test results from all completed LBF testing are described in this section. Results are divided into sections that are based on the procedure used for saturation.

3.1.3.1 LBF Preliminary Specimen Preparation

An LBF specimen (GS-LB01) was prepared as described in Section 2.1 to develop preparation procedures for light backfill triaxial specimens since a standardized sample did not exist at the time of testing. This specimen was considered a practice specimen and was not subjected to consolidation or shearing testing.

3.1.3.2 LBF Tests With Constant Volume Saturation

Saturation using a steel sleeve with and without axial restraint was applied to LBF specimens GS-LB02 and GS-LB03. Saturation data is shown for specimens GS-LB02 and GS-LB03 in Figures 1 and 2, respectively. Figure 2 also includes the axial load reaction that was measured during the constant volume phase. In both Figures 1 and 2, water initially flows into specimens at a relatively high rate and then decreases with time. Once the steel sleeve is removed, the water flow rate increased again and then levelled off once more. Due to difficulties in removal of the sleeve without specimen disturbance and in the interpretation of saturation, this saturation procedure was discontinued.

3.1.3.3 LBF Tests With Constant Mean Effective Stress Saturation

LBF specimen GS-LB04 was saturated at a mean effective stress of 50 kPa followed by an initial consolidation step to 100 kPa. Unfortunately, a leak was discovered during the consolidation phase and the specimen had to be abandoned.

LBF specimen GS-LB05 was subjected to saturation at a mean effective stress of 50 kPa followed by consolidation at 200 kPa, 400 kPa and 800 kPa effective stress levels. Saturation data is shown in Figure 3 while consolidation data for all three consolidation stress levels is plotted in Figure 4. Very little water was removed from the specimen during the 200 kPa consolidation phase. However, similar amounts (~22 mL) were removed during both the 400 kPa and 800 kPa phases. The time from installation until the end of 800 kPa consolidation was a total of two months.

Shearing of specimen GS-LB05 followed consolidation. However, a mechanical restraint in the testing system was accidentally left in place during the initial phase therefore peak and post peak data were not available for this test. The shear phase was completed over one (1) day. Residual strength data were obtained following identification of the testing problem and are plotted in Figures 5, 6 and 7. Deviator stress (q) versus axial strain (ϵ_a), change in pore pressure (u) versus axial strain (ϵ_a), and deviator stress (q) versus mean effective stress (p') are plotted, respectively. From the graphs, it appears that 'critical state' was reached during the shearing phase as deviator stress and pore pressures are not changing significantly with additional axial strain.

3.1.3.4 LBF Tests With Increasing Mean Effective Stress Saturation

LBF specimens GS-LB06, GS-LB07 and GS-LB08 were subjected to saturation under increasing mean stresses up to 350 kPa. Saturation data for the three specimens are shown in Figures 8, 9 and 10, respectively. Following saturation, GS-LB06 was consolidated to 400 kPa, a process that took a total of 95 days (as shown in Figure 11).

Shear data from LBF specimen GS-LB06 including deviator stress versus axial strain, change in pore pressure versus axial strain, and deviator stress versus mean effective stress is provided in Figures 12, 13 and 14, respectively. Using ASTM D 4767, a shear phase of 500 days was calculated based on the length of time to 50% consolidation and assumed peak deviatoric stress at 4% axial strain. The shear phase recommended by ASTM D 4767 was considered unachievable so it was completed over a 1-week period (which is a typical duration used for drained shearing of low conductivity clays). At approximately 8% axial strain, pressurized air supply was lost in the laboratory and back pressure dropped to zero. Once this was discovered it was decided that the best option was to increase back pressure to the initial level and continue with the shearing phase. Figure 13 shows the drop in back pressure that occurred and Figure 14 shows the increase in mean effective stress that resulted. Large-strain data are available from this specimen and 'critical state' can be interpreted for this individual test. However, the results of this test were not included in the deviator stress versus mean effective stress plots used for strength envelope determination.

3.1.3.5 LBF Tests With Direct Pressure Saturation

LBF specimens GS-LB09, GS-LB10, GS-LB11, GS-LB12, GS-LB14, GS-LB15, JB-LB16, and JB-LB17 were brought directly to their desired mean effective stress levels following installation

in the triaxial cell. This series of tests was used to define the strength envelope for LBF and allowed determination of deformation parameters.

Complete saturation data for these specimens is shown in Figures 15 to 22. The saturation designation numbers in the figures refer to the number of times the specimen was installed. Initial saturation (Saturation #1) generally took place in one triaxial cell and then the specimen was transferred to a shearing cell. Prior to shearing, the specimens were allowed to stabilize with respect to volume (Saturation #2).

Following saturation and consolidation, the specimens underwent shearing at a rate of 0.0021 mm/min (20% strain in 7 days). Shear response curves are separated into drained and undrained groups. Deviator stress versus axial strain and deviator stress versus mean effective stress plots for the drained tests are shown in Figures 23 and 24, respectively. Deviator stress versus axial strain and deviator stress versus mean effective stress plots for the undrained tests are shown in Figures 25 and 26, respectively. Figure 27 shows the shear response of all specimens in deviator stress versus mean effective stress space. Volume change during shearing is plotted for the drained tests. This information is shown in Figures 28 to 31, for the 400 kPa, 800 kPa, and two 1,200 kPa drained tests, respectively.

3.1.4 LBF Strength and Deformation Parameters

Table 3 provides a summary of strength and deformation parameters for LBF prepared with freshwater as the pore fluid. Deformation parameters include the Bulk Modulus (K) and Young's Modulus (E). Strength parameters include the critical state strength envelope (M) and the corresponding friction angle at critical state (Φ'_{cs}).

The Bulk Modulus for LBF was determined from the slope of the mean effective stress versus specific volume plot provided in Figure 32. Since consolidation of each specimen was completed in one step, the plot in Figure 32 was constructed by combining the results of the end-of-consolidation specific volumes. The results indicate a Bulk Modulus of 2.8 MPa for the LBF over the specific volume range of 2.2 to 2.6.

Young's Modulus is determined from the slope of the elastic region in a stress-strain plot, prior to yielding of the specimen. Typically, the slope is determined at a point approximately half way between the start of a test and the yield point. It is appropriate to use only the results from the drained tests in order to obtain a true stiffness of the material (i.e. the q - ε_a plots provided in Figure 23). As expected, consolidation to higher pressures increased the stiffness. Young's Modulus values ranged from 120.3 MPa for the specimen consolidated to 400 kPa, to 182.4 MPa for one of the specimens consolidated to 1,200 kPa. The average Young's Modulus for all of the drained tests conducted on LBF is 155.9 MPa.

According to elastic theory, Poisson's Ratio can be determined if the Bulk Modulus and Young's Modulus are known. However, the above values do not result in a reasonable Poisson's Ratio. There appears to be a disconnect in the independent determination of these two parameters (i.e. the consolidation phase from combined data was used to determine the Bulk Modulus, and the shearing phases of the drained tests were used to determine Young's Modulus). Greater confidence is given to the Young's Modulus determination since the data required for that parameter is obtained over a shorter duration with higher quality measurements. Determination of the bulk Modulus employed manually read data over a long duration. The long duration may introduce errors in the actual amount of water being measured in the backpressure burettes

relative to the actual amount being expelled from the specimen. Any minute leak in the triaxial testing system will result in more water being observed in the burettes than is actually being expelled from the specimen. This will give the appearance of a material with lower stiffness (i.e. lower Bulk Modulus) than the actual case. Further investigation is required to determine the source of this disconnect. Sacrificial tests (where multiple specimens are consolidated to different pressures in triaxial chambers and then removed from the apparatus for mass and volume measurements) may provide further insight and a more reliable Bulk Modulus value.

Since the LBF material displays marked strain softening, the peak strengths for each consolidation pressure are included in Table 3. This behaviour results in an 'over-consolidated' region where the peak strengths are significantly higher than the critical state strength envelope, especially at lower consolidation pressures. The shape of the peak values in Figure 27, combined with the strain softening behaviour, suggests that an anisotropic elastic-plastic constitutive model can describe the material behaviour. As such, a complete analysis using an elastic-plastic framework is warranted for this material once the results of the specimens prepared with saline pore fluid are available for comparison.

The strength of a clay material can be defined using the critical state strength envelope. This strength envelope is shown as the critical state line (CSL) in Figure 27. The slope of the CSL defines the strength envelope and is known as the strength parameter, M . Critical state, M , values were also calculated for each individual test (Table 3). This value is obtained from the ratio of $q-p'$ at critical state (stabilized portion of the stress-strain curve after strain-softening). The average of all tests is 0.51, which is close to the value obtained from the slope of the CSL (0.47) shown in Figure 27. The corresponding critical state friction angle is 13.5° . This value indicates that the strength of the LBF is similar to that of a natural glacial lake clay (e.g. Lake Agassiz Clay, $\Phi'_{cs} = 13^\circ$, Man 2006) and that of BSB ($\Phi'_{cs} = 14^\circ$, Graham et al. 1989).

3.2 DENSE BACKFILL (DBF) TESTS (UNIVERSITY OF MANITOBA)

3.2.1 DBF Test Program

Table 2 summarizes the tests that have been conducted on DBF as part of this contract. The testing program included testing at three different isotropic consolidation pressures (400 kPa, 800 kPa and 1,200 kPa).

3.2.2 DBF Test Procedure

Similar to the tests conducted on LBF, the procedures outlined in ASTM D 4767- Consolidated Undrained Triaxial Compression Test for Cohesive Soils (1995), were generally followed for all tests conducted on DBF. Specimens were immediately brought to their final mean effective stress as described for the LBF specimens. Prepared specimens were provided by AECL, as such, besides trimming, no preparation was required prior to installation.

3.2.3 DBF Test Results

DBF specimens JB-DBF13, JB-DBF14, GS-DBF15, JB-DBF16, GS-DBF17, GS-DBF18, GS-DBF19 and GS-DBF20 were brought directly to their desired mean effective stress levels following installation in the triaxial cell. Complete saturation data for these specimens is shown in Figures 33 to 40. As for the LBF specimens, the saturation designation numbers in the figures refer to the number of times the specimen was installed into a triaxial cell, with the second installation corresponding to placement into the shearing cell. Separate cells were used for consolidation and shearing, to prevent specimens with long consolidation times from occupying the shearing apparatus for prolonged periods.

Following saturation and consolidation, the specimens underwent shearing at a rate of 0.0021 mm/min (30% strain in 10 days). Shear response curves are separated into drained and undrained groups. Deviator stress versus axial strain and deviator stress versus mean effective stress plots for the drained tests are shown in Figures 41 and 42, respectively. Deviator stress versus axial strain and deviator stress versus mean effective stress plots for the undrained tests are shown in Figures 43 and 44, respectively. Figure 45 shows the shear response of all specimens in deviator stress versus mean effective stress space. Volume change during shearing is plotted for the drained tests. This information is shown in Figures 46 to 49, for the 400 kPa, 800 kPa and two 1,200 kPa drained tests, respectively.

3.2.4 DBF Strength and Deformation Parameters

Table 4 provides a summary of strength and deformation parameters for DBF prepared with freshwater as the pore fluid. As for the LBF specimens, deformation parameters include the Bulk Modulus (K) and Young's Modulus (E). Strength parameters include the critical state strength envelope (M) and the corresponding friction angle at critical state (Φ'_{cs}).

The Bulk Modulus for DBF was determined from the slope of the mean effective stress versus specific volume plot provided in Figure 50. Since consolidation of each specimen was completed in one step, the plot in Figure 50 was constructed by combining the results of the end-of-consolidation specific volumes. The results indicate a Bulk Modulus of 10.7 MPa for the DBF, which is significantly stiffer than the LBF.

Young's Modulus for the DBF was determined in the same way as described for the LBF specimens, using the deviator stress versus axial strain ($q-\epsilon_a$) plots from the drained test provided in Figure 41. Consolidation to higher pressures increased the stiffness. Young's Modulus values ranged from 124.7 MPa for the specimen consolidated to 400 kPa, to 347.1 MPa for one of the specimens consolidated to 1,200 kPa. The average Young's Modulus for all of the drained tests conducted on DBF is 261.7 MPa.

For the same reasons as discussed for the LBF, a reasonable Poisson's Ratio was not obtained for DBF using the above Bulk Modulus and Young's Modulus. Further testing is required to confirm the Bulk Modulus.

The DBF displayed less strain softening than the LBF. However, the peak strengths for each consolidation pressure are provided in Table 4 for completeness. These values will be close to those used to determine the critical state strength envelope (M) and corresponding friction angle. That is, the peak values are generally close to the critical state strength envelope provided in Table 4 ($\Phi'_{cs} \cong \Phi'_{peak}$). The shape of the peak values in Figure 45 suggests that an

alternative constitutive model to describe the behaviour of DBF would be the Duncan-Chang (1970) nonlinear model for describing strength envelopes. Analysis using the Duncan-Chang model is warranted for this material once the results of the specimens prepared with saline pore fluid are available for comparison.

The critical state strength envelope for the DBF is shown in Figure 45. Critical state, M , values were also calculated for each individual test (Table 4). The average M value for all of the tests is 1.12, which is close to the value obtained from the slope of the CSL (1.10) shown in Figure 45. The corresponding critical state friction angle is 28° , indicating that the DBF is significantly stronger than the LBF.

4. STATUS OF TRIAXIAL TESTING OF LBF AND DBF WITH SALINE PORE FLUID

Work in 2007 is a continuation of previous investigations examining the stress-strain behaviour of LBF and DBF, only now containing saline water as the pore fluid. The matrix of tests to be completed with saline pore fluid is the same as for the initial program with fresh water as the pore fluid (Tables 1 and 2).

The Royal Military College of Canada (RMC) in Kingston, ON has commissioned two (2) high-pressure triaxial cells obtained from the University of Manitoba. The cells were refurbished and upgraded to allow for use of saline solutions as the pore fluid.

The primary objective of the continued investigations is to examine the influence of pore fluid chemistry on the stress-strain behaviour of LBF and DBF. The above-reported work, completed at the University of Manitoba, has examined the stress-strain behaviour of LBF and DBF using Distilled De-aired Water (DDW) as a mixing fluid and saturation fluid. The continuing investigations include completion of similar traditional triaxial tests using a saline solution (250 g/L CaCl_2) as a mixing fluid and pore fluid for saturation. The tests to be conducted at RMC will be used to establish preliminary parameters relating to compressibility, strength, unit weight, stress history, yielding and failure with saline pore fluid. The tests include drained and undrained triaxial tests at isotropic compression levels of 400 kPa, 800 kPa and 1,200 kPa. Repeat tests are included to give higher confidence in the results since these are the first traditional triaxial tests to be completed with saline pore fluid on these materials. Following tests, strength and stiffness parameters will be interpreted for LBF and DBF and compared with similar parameters interpreted from tests using freshwater.

Two (2) triaxial tests on light backfill have been initiated: a 400 kPa consolidated undrained triaxial test (LBF-1004); and an 800 kPa consolidated undrained triaxial test (LBF-1006). The two test specimens were prepared using 250 g/L CaCl_2 pore fluid to a target water content and dry density of 14.4% and 1.24 Mg/m^3 respectively. The two test specimens are currently in the saturation phase as shown in Figures 51 and 52. Following standard procedures, the saturation phase will continue until a B Test of 0.95 or greater is achieved (Note: a B test is conducted by increasing the cell pressure with drainage from the specimen closed. The increase in pore pressure is subsequently measured, and the B value is determined by dividing the increase in pore pressure by the increase in cell pressure.). Following saturation, the test specimens will be sheared at similar strain rate as applied in the freshwater tests on LBF.

5. SUMMARY

Preliminary triaxial strength testing has been performed on light backfill (LBF) and dense backfill (DBF) materials using freshwater as the pore fluid. The triaxial strength testing has provided insight into the behaviour of both of these materials. Results of the testing program allowed determination of strength and deformation (stiffness) parameters for both materials. Deformation parameters included the Bulk Modulus and Young's Modulus. Strength parameters included the critical state strength envelope and corresponding friction angle. The test results can also be used as a database for determining strength and deformation parameters for alternative constitutive models that may be used in the modeling of these materials.

The LBF displayed brittle, strain-softening behaviour with what appears to be an asymmetrical yield locus, similar to natural clays. A complete analysis using an elastic-plastic framework is warranted for this material once the results of the specimens prepared with saline pore fluid are available for comparison. The Bulk Modulus for the LBF is 2.8 MPa and the average Young's Modulus for the material is 155.9 MPa. The critical state strength envelope for the LBF has a slope of $M = 0.47$, with a corresponding critical state friction angle of 13.5° . The strength envelope of the LBF is also similar to that of natural glacial lake clays (for example Glacial Lake Agassiz Clay, $\Phi'_{cs} = 13^\circ$) and that of bentonite-sand buffer (BSB, $\Phi'_{cs} = 14^\circ$).

In comparison, the DBF displayed less brittle (more ductile) behaviour than the LBF. As expected, the DBF is significantly stronger and stiffer than the LBF. The Bulk Modulus for the DBF is 10.7 MPa and the average Young's Modulus for the material is 261.7 MPa. The critical state strength envelope for the DBF has a slope of $M = 1.10$, with a corresponding critical state friction angle of 28° . An alternative constitutive model to describe the behaviour of DBF would be the Duncan-Chang model.

According to elastic theory, Poisson's Ratio can be determined if the Bulk Modulus and Young's Modulus are known. However, the above values do not result in reasonable Poisson's Ratios. It is suspected that the Bulk Modulus values are artificially low due to small amounts of error introduced by the method of determination. Sacrificial specimens, consolidated to different pressures would avoid such errors and allow confirmation of the Bulk Modulus. At this stage, greater confidence is given to the Young's Modulus values presented in this report.

Many lessons have been learned during LBF testing that resulted in the improvement of testing procedures. The unexpectedly low hydraulic conductivity of both materials significantly increased the time required for testing. It was found that performing saturation and consolidation in one increment allows tests to be completed in a reasonable timeframe. Strength and deformation results should not be significantly affected by the direct saturation method.

The next step will be to compare the results of this preliminary program to the same series of test conducted using saline water as the pore fluid. This will be done in 2008 and will aid in the design and analysis of potential repository placement within sedimentary rocks.

REFERENCES

- AECL (Atomic Energy of Canada Limited). 1994. Environmental impact statement on the concept for disposal of Canada's nuclear fuel waste. Atomic Energy of Canada Limited Report, AECL-10711, COG-93-1.
- ASTM D 4767. 1995. Consolidated undrained triaxial compression test for cohesive soils. ASTM, Philadelphia, Pennsylvania, USA.
- Baumgartner, P. 1996. A used-fuel repository with the in-room emplacement method: Integration in the design process. In Proc. International Conference on Deep Geological Disposal of Radioactive Waste, Winnipeg, Manitoba, 1996 September 16-19.
- Duncan, J.M. and Chang, C.Y., 1970. Nonlinear analysis of stress and strain in soils. Journal of the Soil Mechanics and Foundations Division, ASCE, Vol. 96, No. SM5, pp. 1629-1654.
- Graham, J., F. Saadat, M.N. Gray, D.A. Dixon, Q.Y. Zhang. 1989. Strength and volume change behaviour of a sand-bentonite mixture. Can. Geotech. J. 26, 292-305.
- Johnson, L.H., D.M. LeNeveu, D.W. Shoesmith, D.W. Oscarson, M.N. Gray, R.J. Lemire and N. Garisto. 1994. The disposal of Canada's nuclear fuel waste: The vault model for post-closure assessment. Atomic Energy of Canada Limited Report, AECL-10714, COG-93-4.
- Maak, P. and G.R. Simmons. 2005. Deep geologic repository concepts for isolation of used fuel in Canada. In Proc. Canadian Nuclear Society conference Waste Management, Decommissioning and Environmental Restoration for Canada's Nuclear Activities: Current Practices and Future Needs. 2005 May 8-11, Ottawa.
- Man, A.G. 2006. The effect of changes in pore fluid geochemistry on the elastic-plastic behaviour of Lake Agassiz Clay. Ph.D. Thesis, Department of Civil Engineering, University of Manitoba, Winnipeg, Manitoba.
- Mazurek, M. 2004. Long-term used nuclear fuel waste management – Geoscientific review of the sedimentary sequence in southern Ontario. Institute of Geological Sciences, Univ. of Bern, Technical Report TR 04-01, Bern, Switzerland, available from Nuclear Waste Management Organization, Toronto, Canada (www.nwmo.ca).
- Russell, S.B. and G.R. Simmons. 2003. Engineered barrier system for a deep geologic repository. Presented at the 2003 International High-Level Radioactive Waste Management Conference. 2003 March 30-April 2, Las Vegas, NV.

Table 1: Matrix of Triaxial Tests on LBF

Type of Test	Isotropic Compression Level (kPa)		
	400	800	1,200
Undrained Tests	GS-LB06 GS-LB15	GS-LB09	GS-LB10 JB-LB17
Drained Tests	GS-LB11	GS-LB14	GS-LB12 JB-LB16

Table 2: Matrix of Triaxial Tests on DBF

Type of Test	Isotropic Compression Level (kPa)		
	400	800	1,200
Undrained Tests	GS-DBF19	JB-DBF16	JB-DBF14 GS-DBF17
Drained Tests	GS-DBF15	GS-DBF18	GS-DBF12 GS-DBF13

Table 3: LBF Strength and Deformation Parameters

Specimen	Test Type	Bulk Modulus K (MPa)	Young's Modulus E (MPa)	Peak Strength q (kPa)	Critical State M	Friction Angle Φ'_{cs} (degrees)
LBF Undrained Tests						
GS-LB15	CIŪ @ 400 kPa	-	-	347	0.66	17
GS-LB09	CIŪ @ 800 kPa	-	-	462	0.46	12
GS-LB10	CIŪ @ 1,200 kPa	-	-	742	0.57	15
JB-LB17	CIŪ @ 1,200 kPa	-	-	783	0.51	14
LBF Drained Tests						
GS-LB11	CID @ 400 kPa	Figure 32	120.3	297	0.52	14
GD-LB14	CID @ 800 kPa	Figure 32	145.8	638	0.52	14
GS-LB12	CID @ 1,200 kPa	Figure 32	175.0	663	0.38	10
JB-LB16	CID @ 1,200 kPa	Figure 32	182.4	712	0.42	11
	Average:	2.8	155.9		0.51	14
	From Figure 27:				0.47	13

Table 4: DBF Strength and Deformation Parameters

Specimen	Test Type	Bulk Modulus	Young's Modulus	Peak Strength	Critical State	Friction Angle
		K (MPa)	E (MPa)	q (kPa)	M	Φ'_{cs} (degrees)
DBF Undrained Tests						
GS-DBF19	CIŪ @ 400 kPa	-	-	715	1.18	30
JB-DBF16	CIŪ @ 800 kPa	-	-	901	1.16	29
	CIŪ @ 1,200					
GS-DBF17	kPa	-	-	1,131	1.32	33
	CIŪ @ 1,200					
JB-DBF14	kPa	-	-	1,334	1.10	28
DBF Drained Tests						
GS-DBF15	CID @ 400 kPa	Figure 50	124.7	789	1.07	27
GS-DBF18	CID @ 800 kPa	Figure 50	230.9	1,483	1.11	28
GS/JB-DBF13	CID @ 1,200 kPa	Figure 50	344.0	1,843	0.95	24
GS/JB-DBF12	CID @ 1,200 kPa	Figure 50	347.1	2,220	1.06	27
	Average:	10.7	261.7		1.12	28
	From Figure 45:				1.10	28

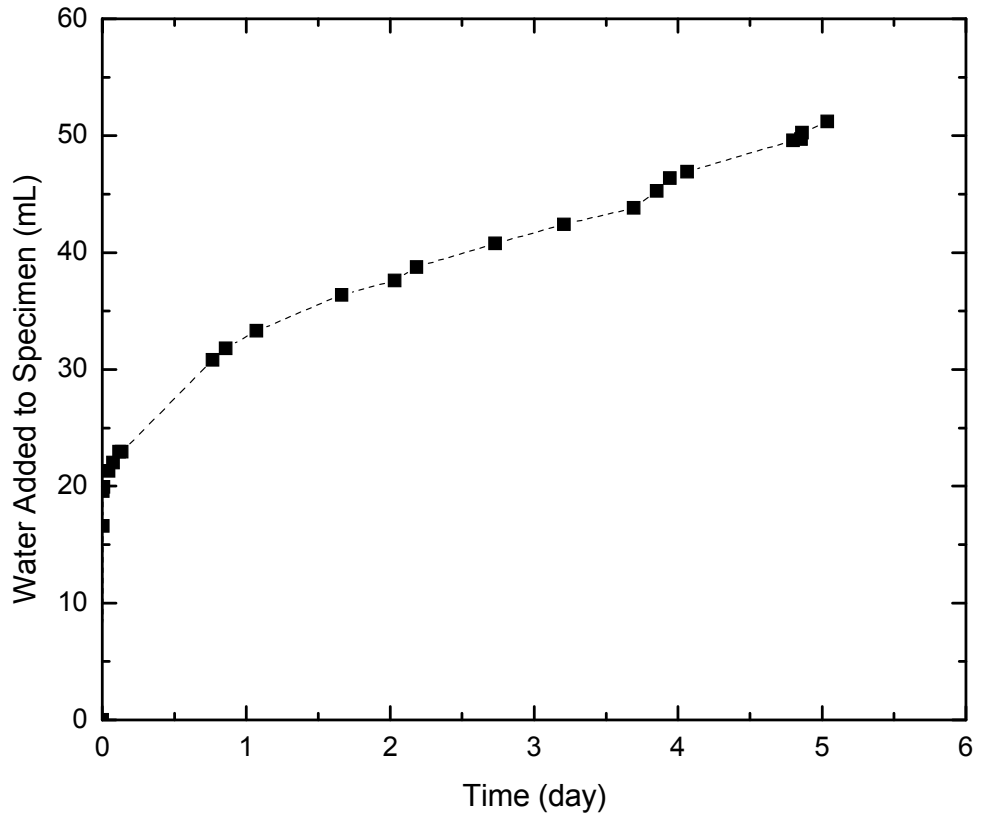


Figure 1: LBF Specimen GS-LB02: Saturation Phase (sleeve not removed)

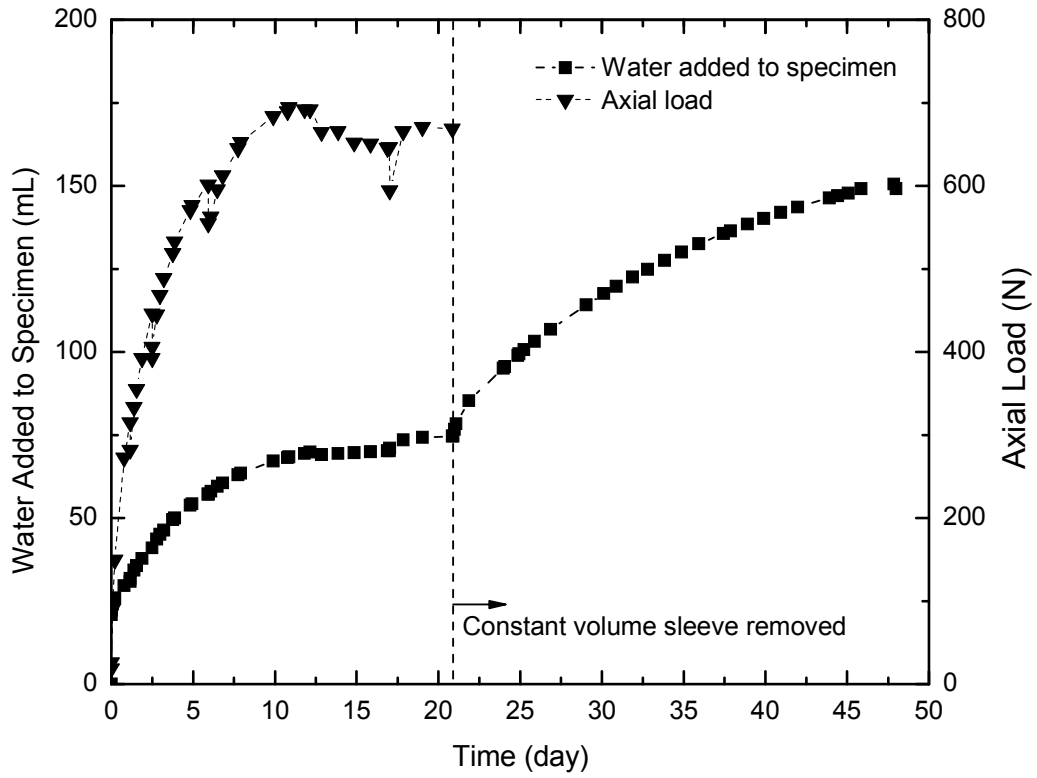


Figure 2: LBF Specimen GS-LB03: Saturation Phase

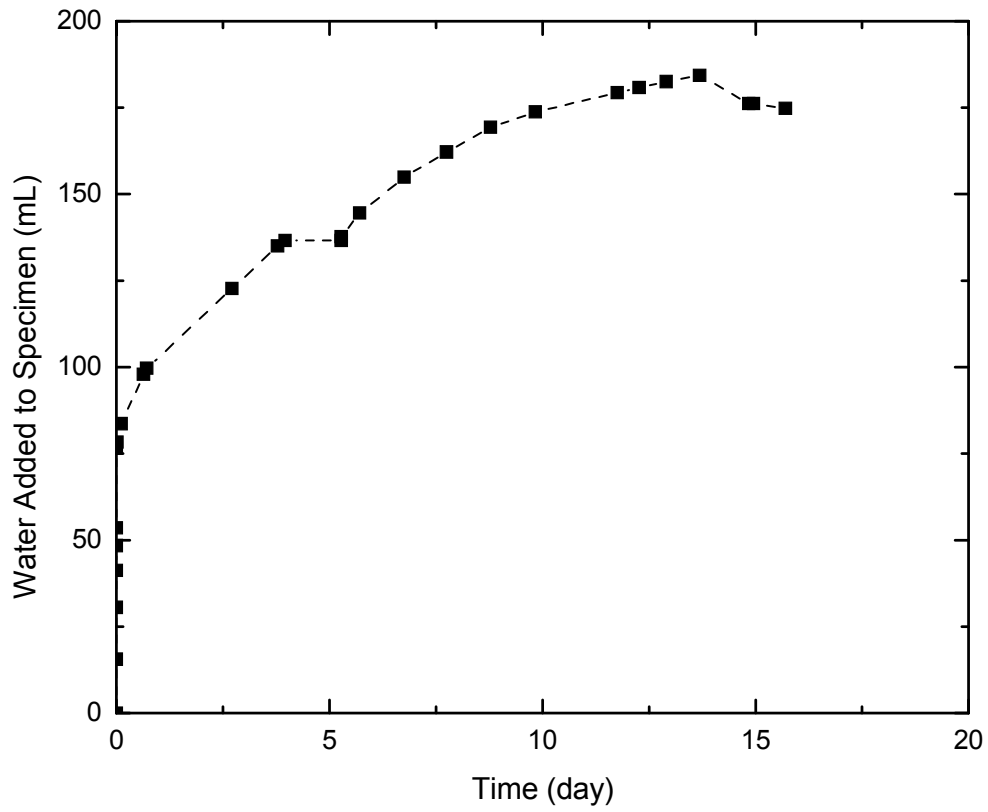


Figure 3: LBF Specimen GS-LB05: Saturation Phase

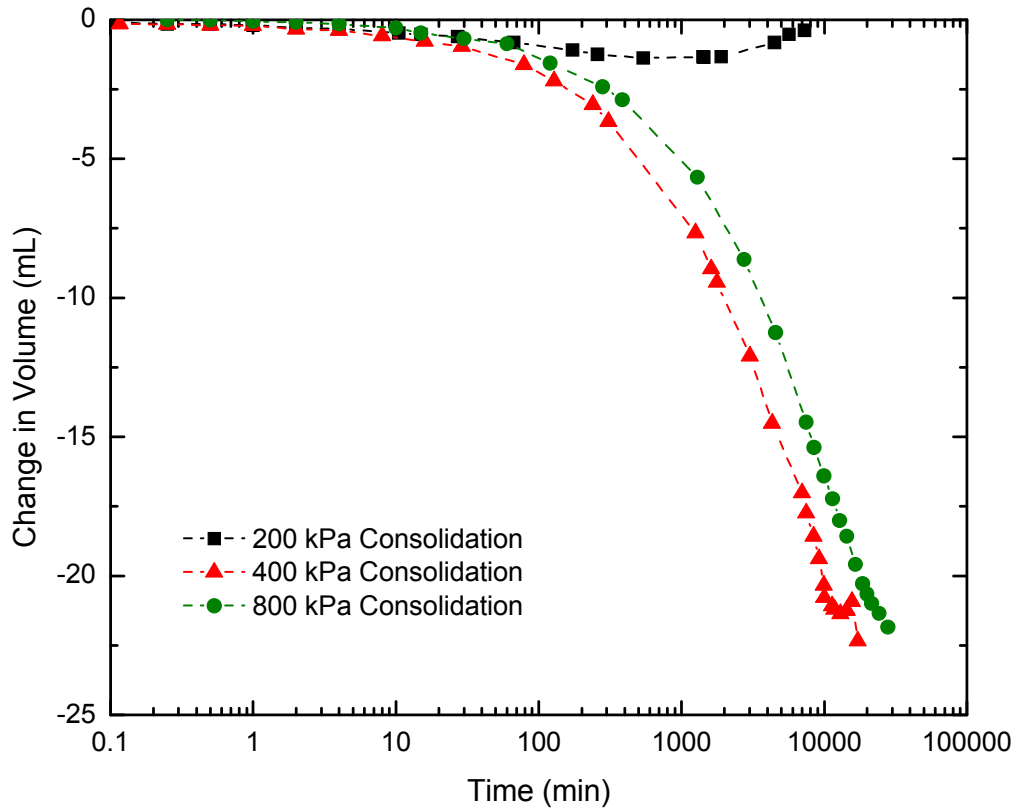


Figure 4: LBF Specimen GS-LB05: 200 kPa, 400 kPa and 800 kPa Consolidation Phases

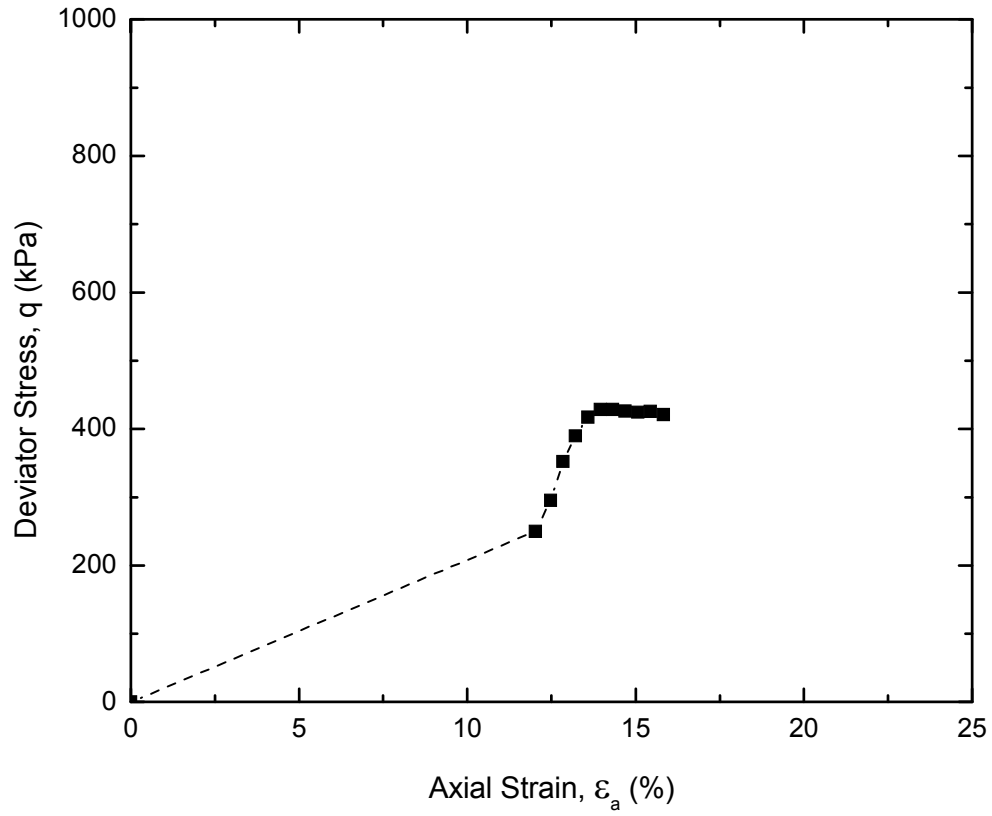


Figure 5: LBF Specimen GS-LB05: Deviator Stress (q) Versus Axial Strain (ϵ_a)

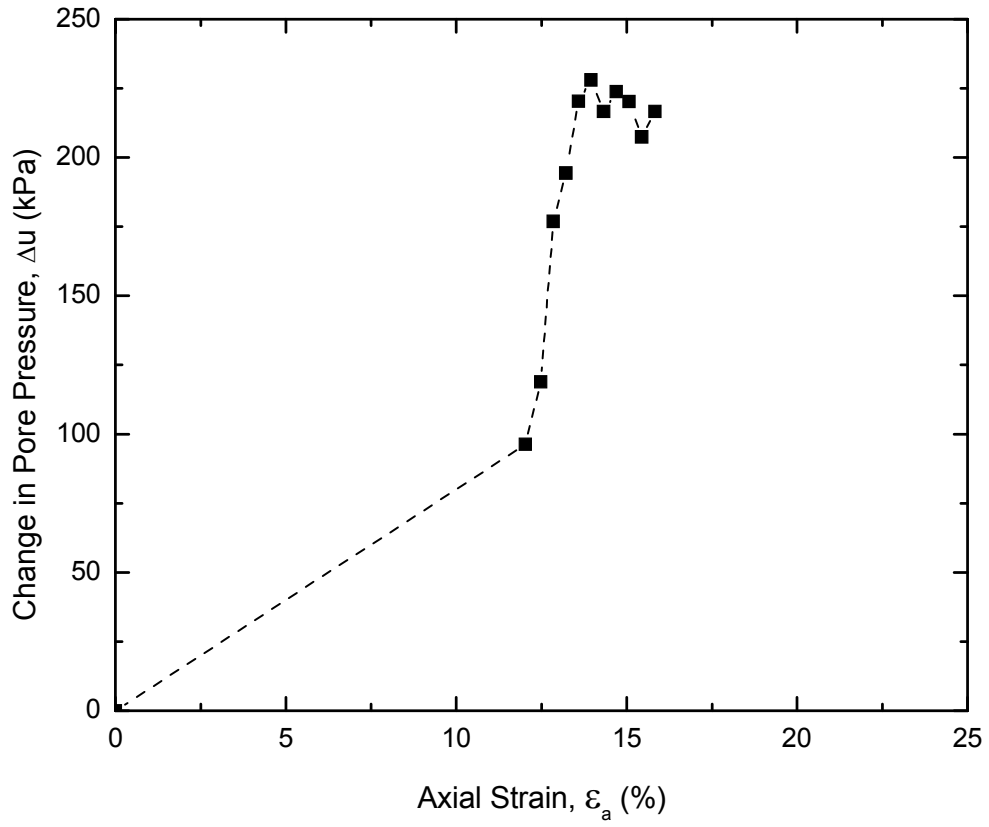


Figure 6: LBF Specimen GS-LB05: Change in Pore Pressure (Δu) Versus Axial Strain (ϵ_a)

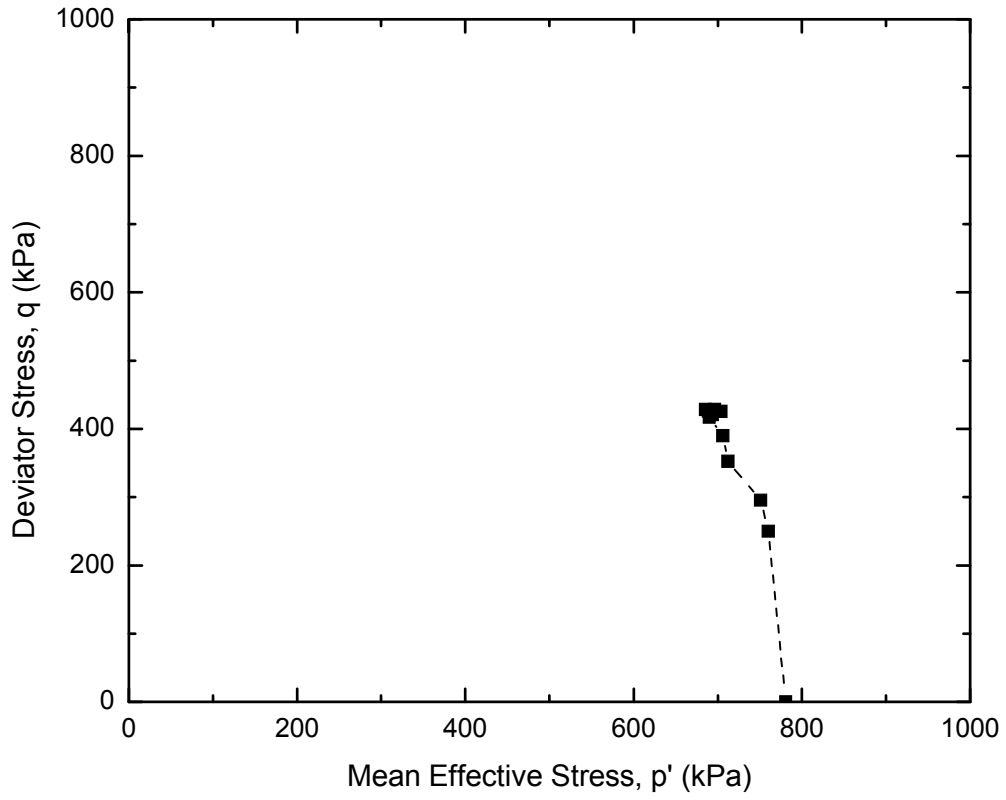


Figure 7: LBF Specimen GS-LB05: Deviator Stress (q) Versus Mean Effective Stress (p')

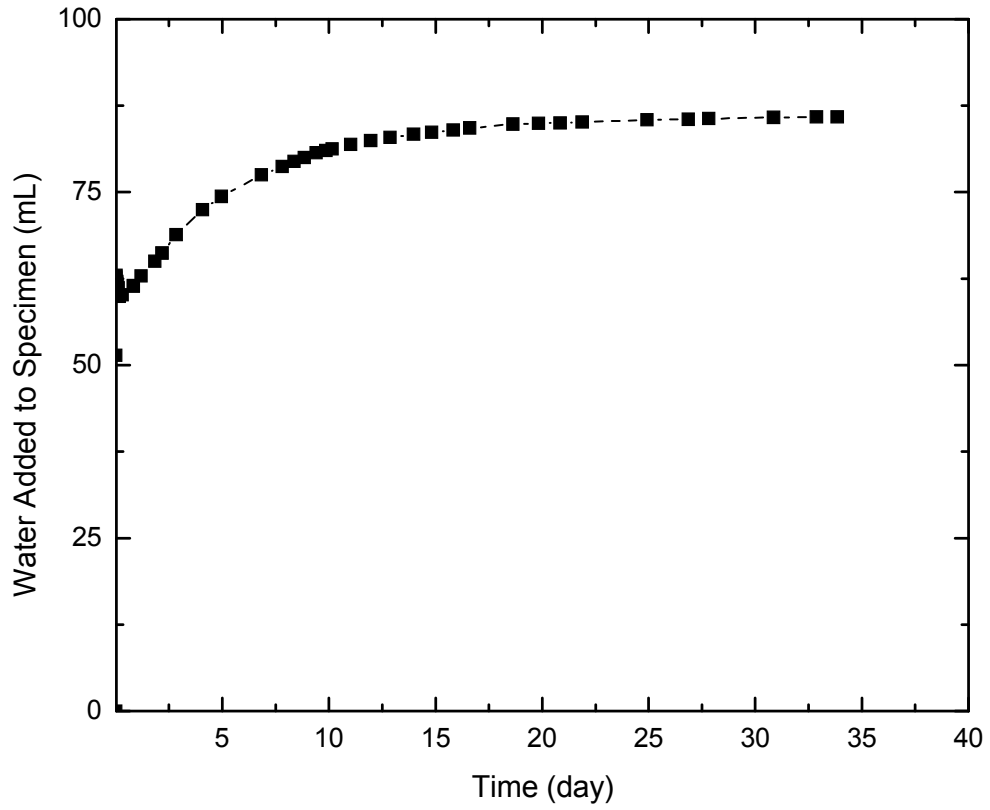


Figure 8: LBF Specimen GS-LB06: Saturation Phase

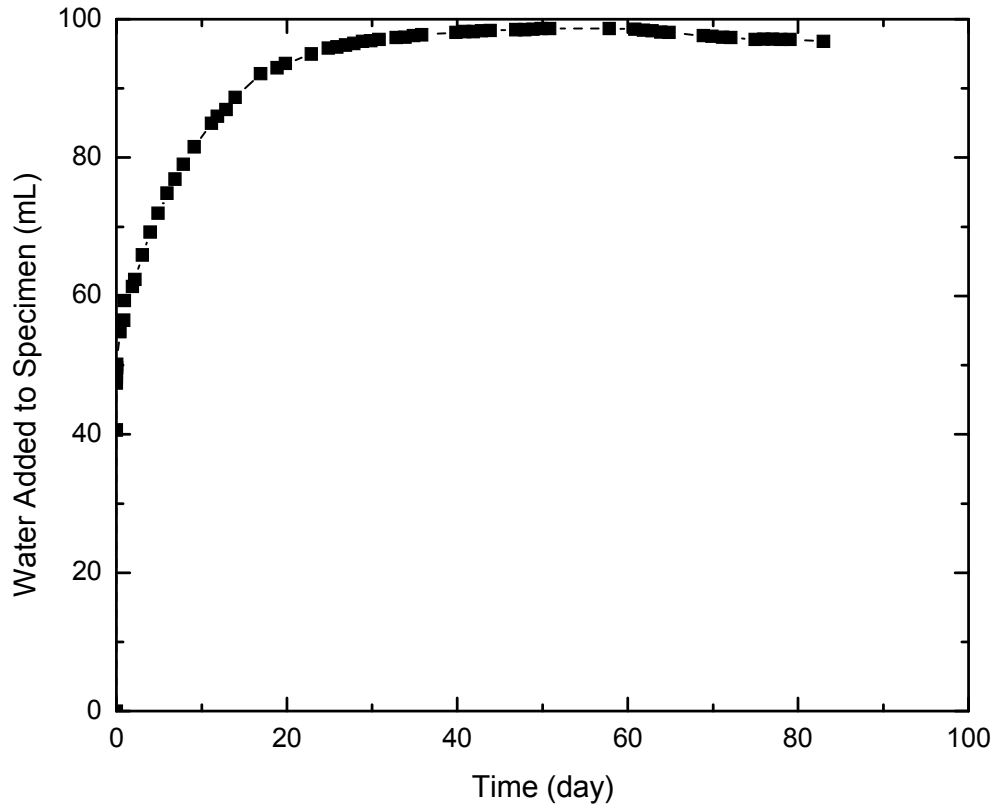


Figure 9: LBF Specimen GS-LB07: Saturation Phase

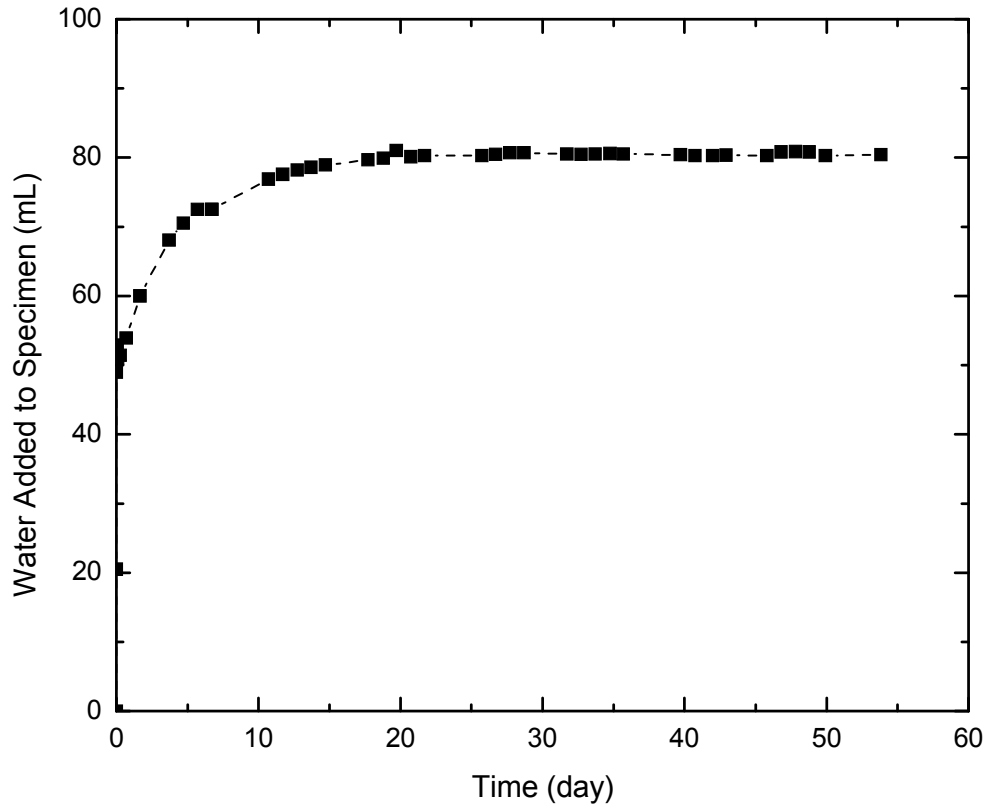


Figure 10: LBF Specimen GS-LB08: Saturation Phase

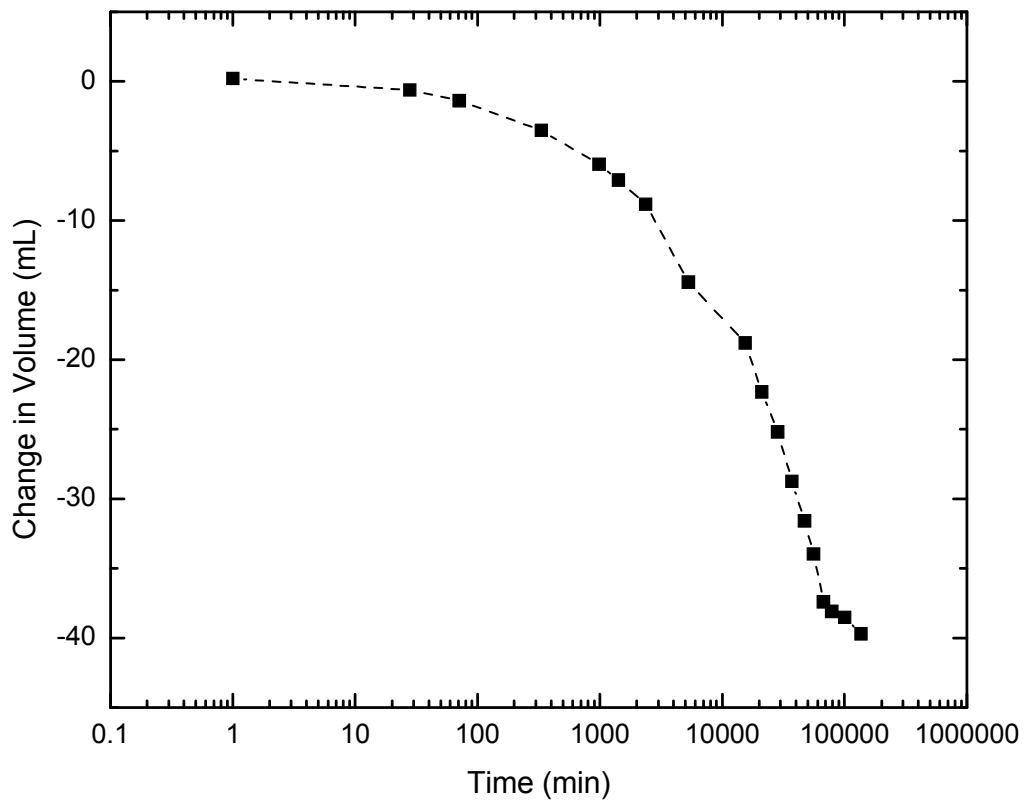


Figure 11: LBF Specimen GS-LB06: 400 kPa Consolidation Phase

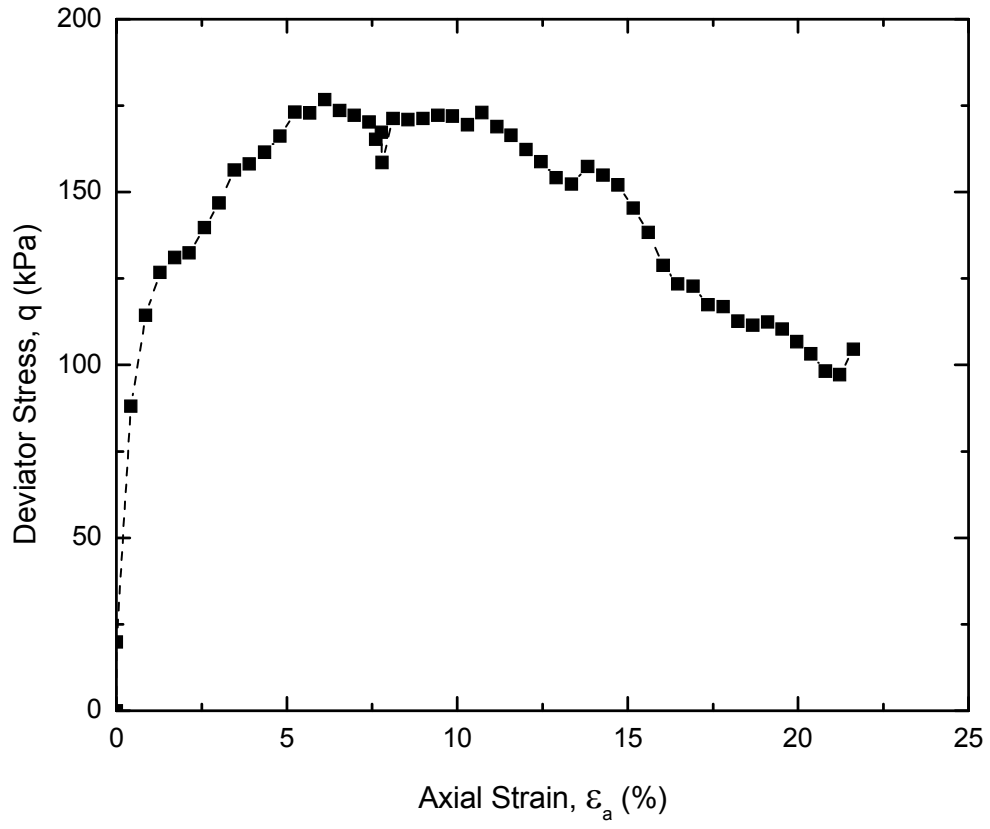


Figure 12: LBF Specimen GS-LB06: Deviator Stress Versus Axial Strain

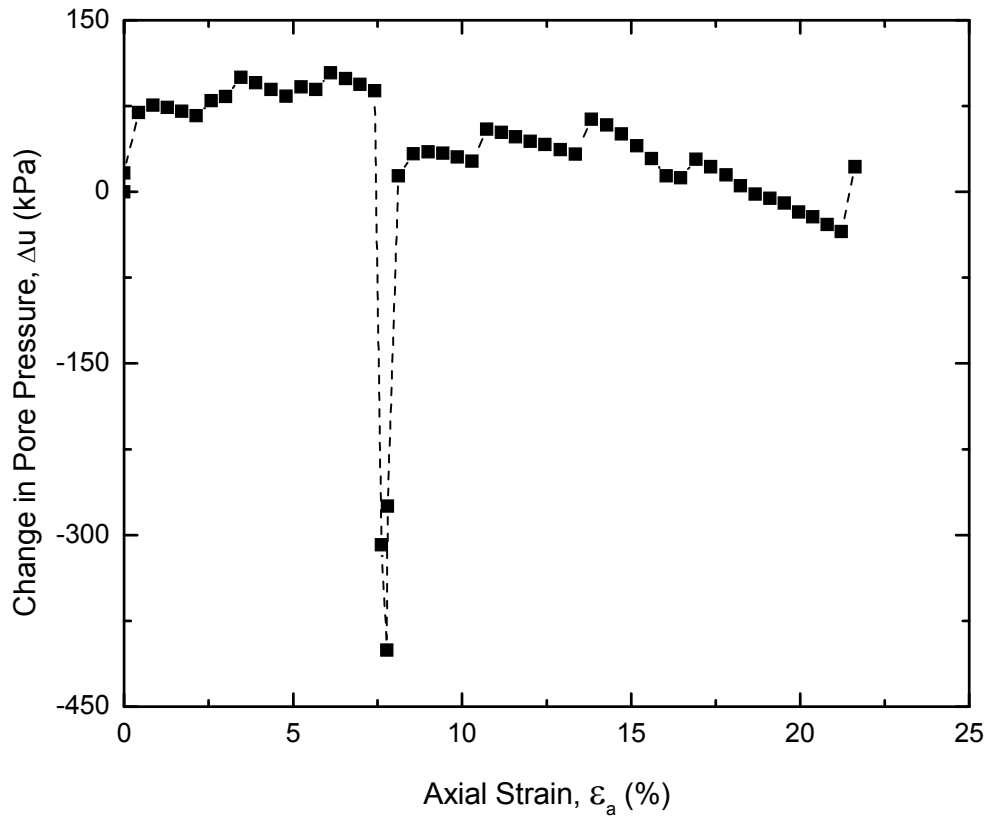


Figure 13: LBF Specimen GS-LB06: Change in Pore Pressure Versus Axial Strain

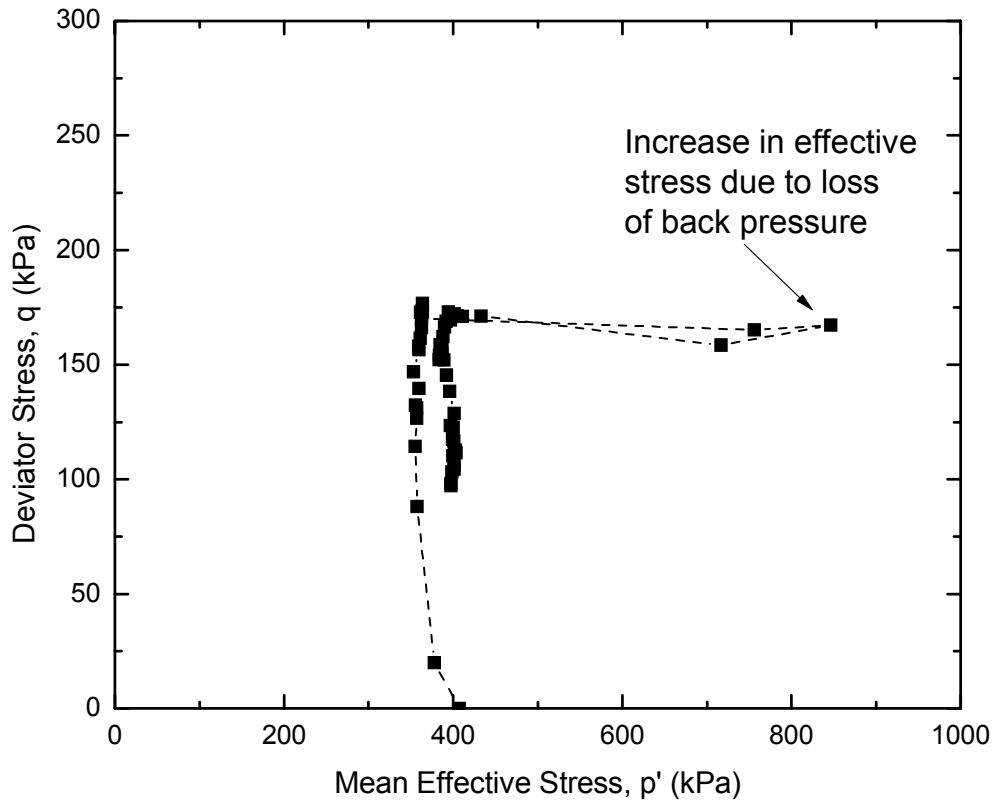


Figure 14: LBF Specimen GS-LB06: Deviator Stress Versus Mean Effective Stress

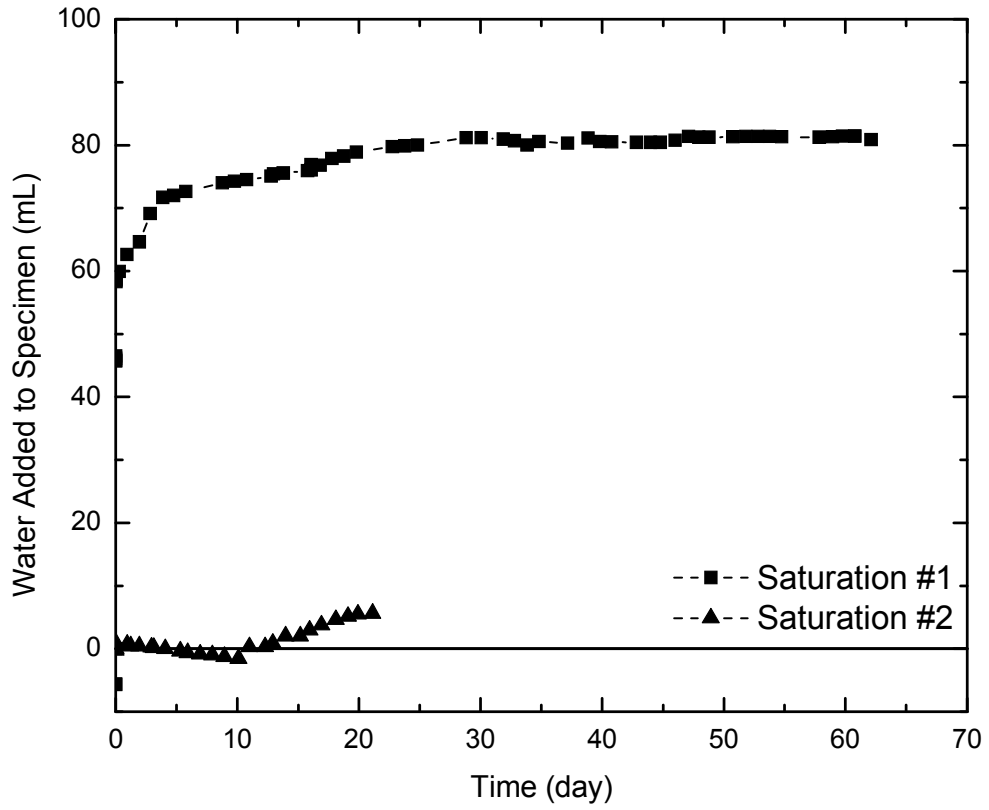


Figure 15: LBF Specimen GS-LB09: Saturation Phases

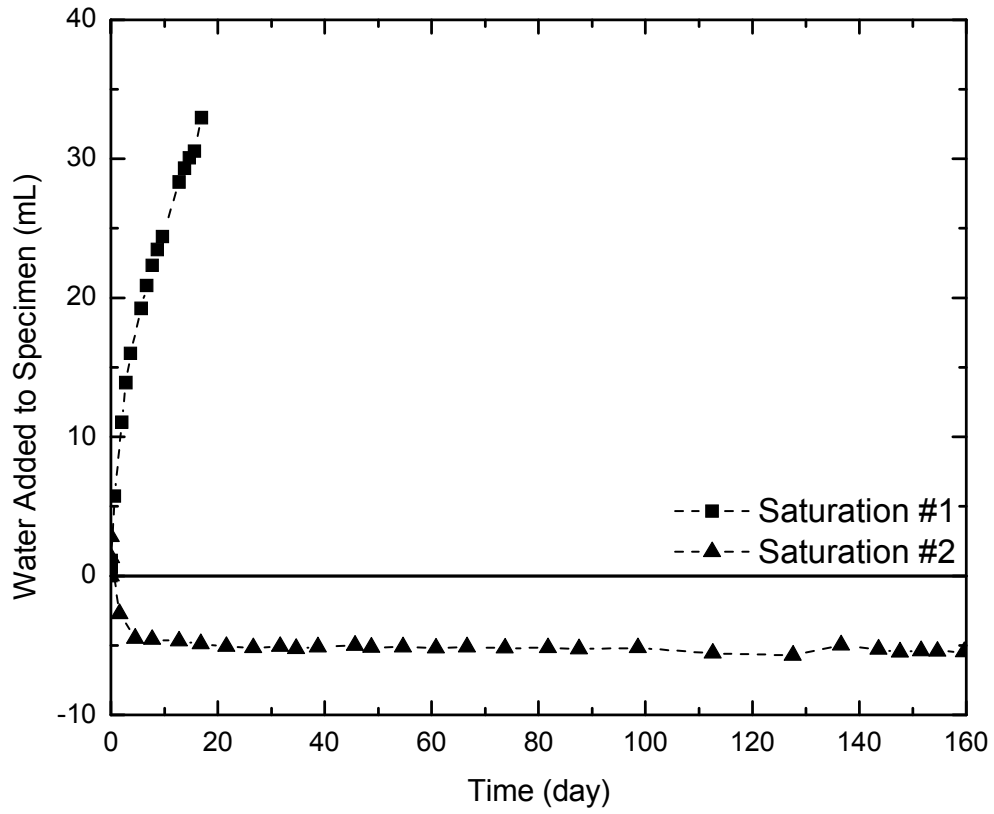


Figure 16: LBF Specimen GS-LB10: Saturation Phases

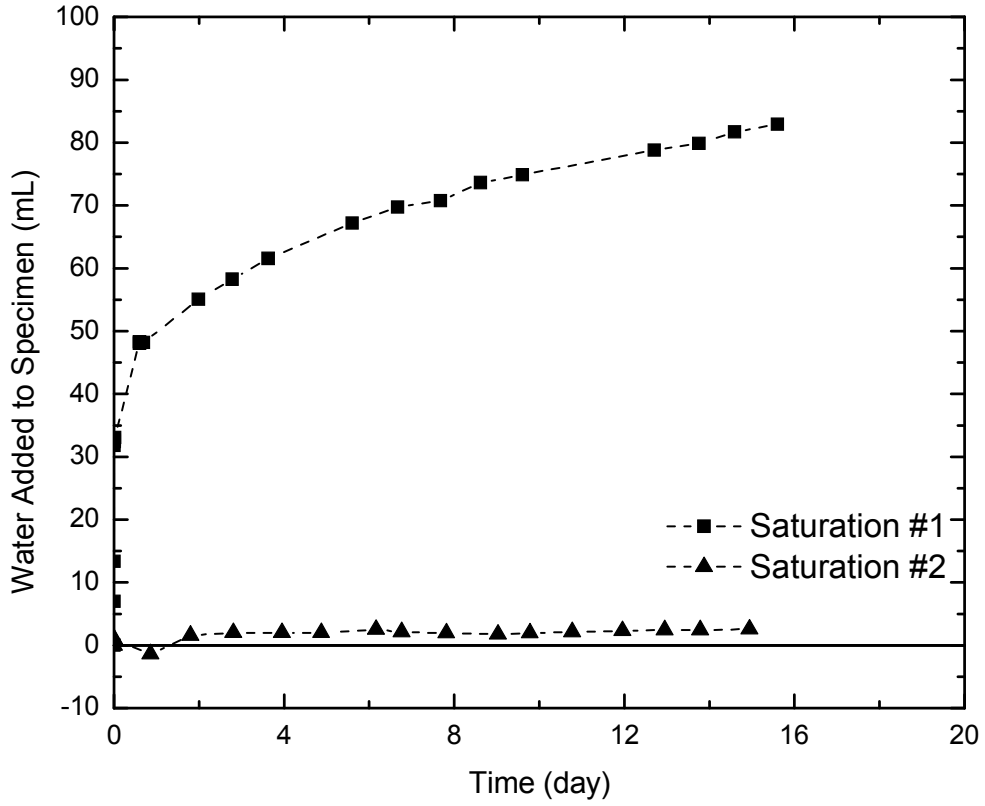


Figure 17: LBF Specimen GS-LB11: Saturation Phases

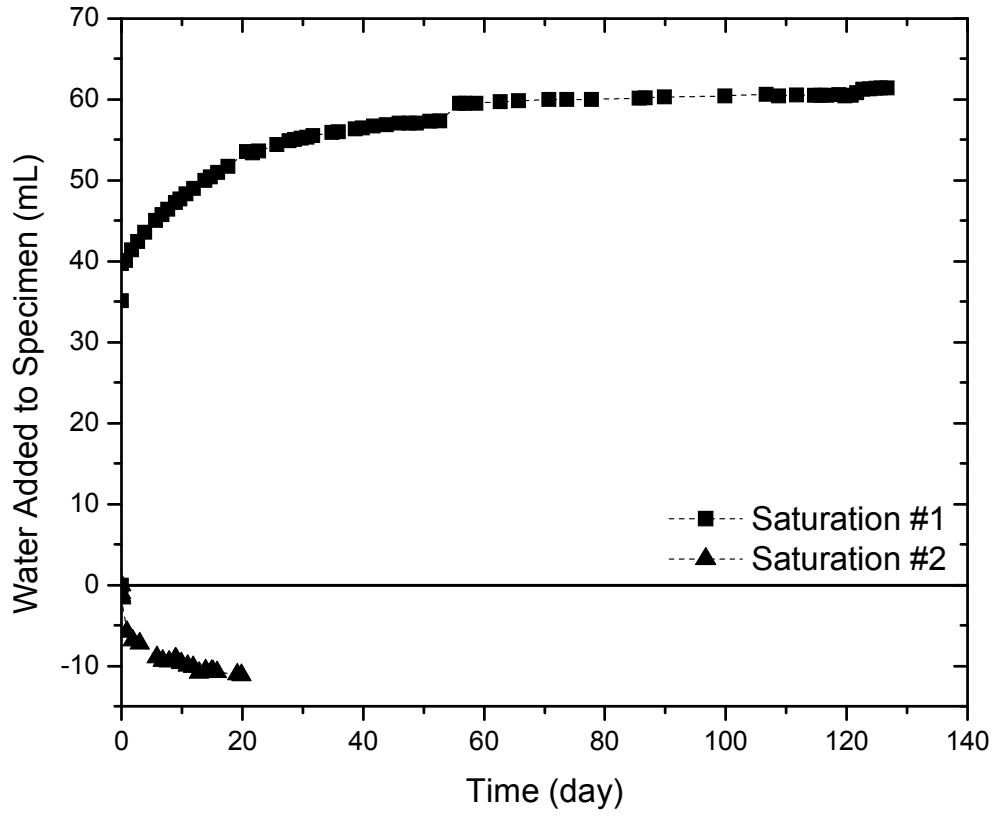


Figure 18: LBF Specimen GS-LB12: Saturation Phases

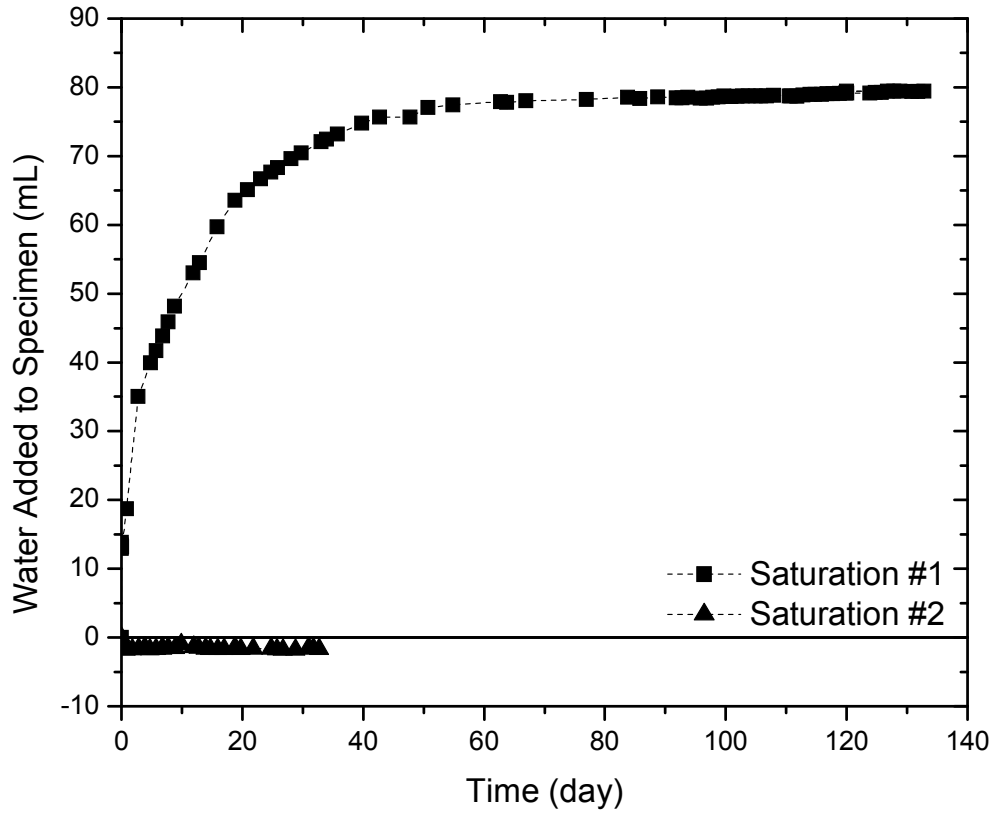


Figure 19: LBF Specimen GS-LB14: Saturation Phases

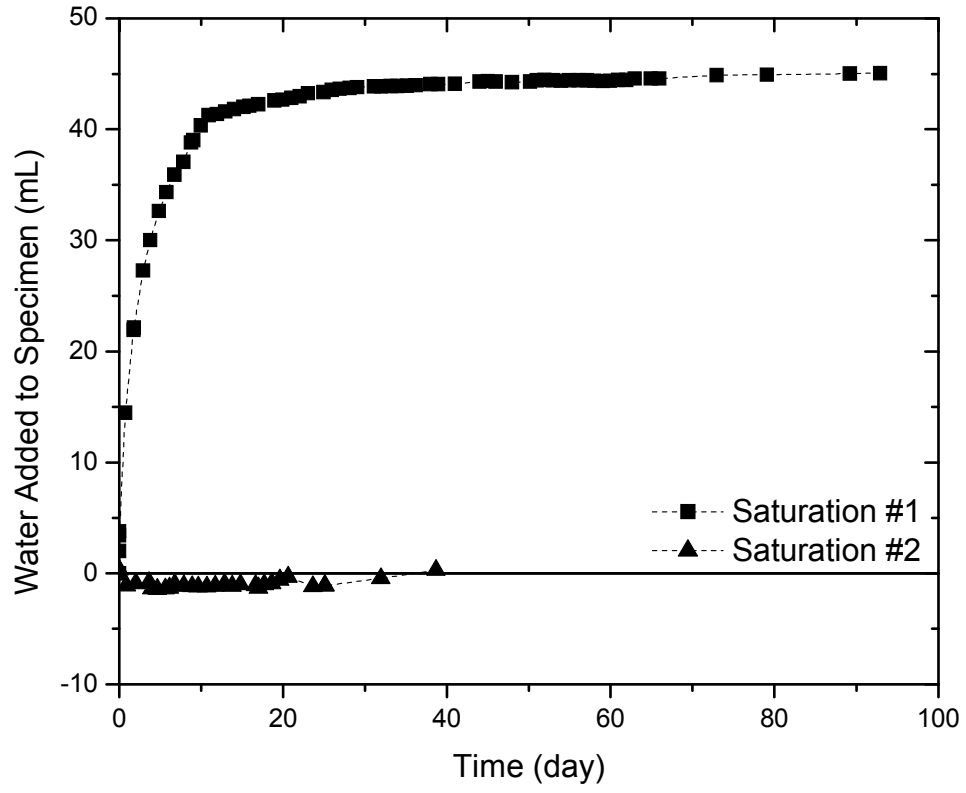


Figure 20: LBF Specimen GS-LB15: Saturation Phases

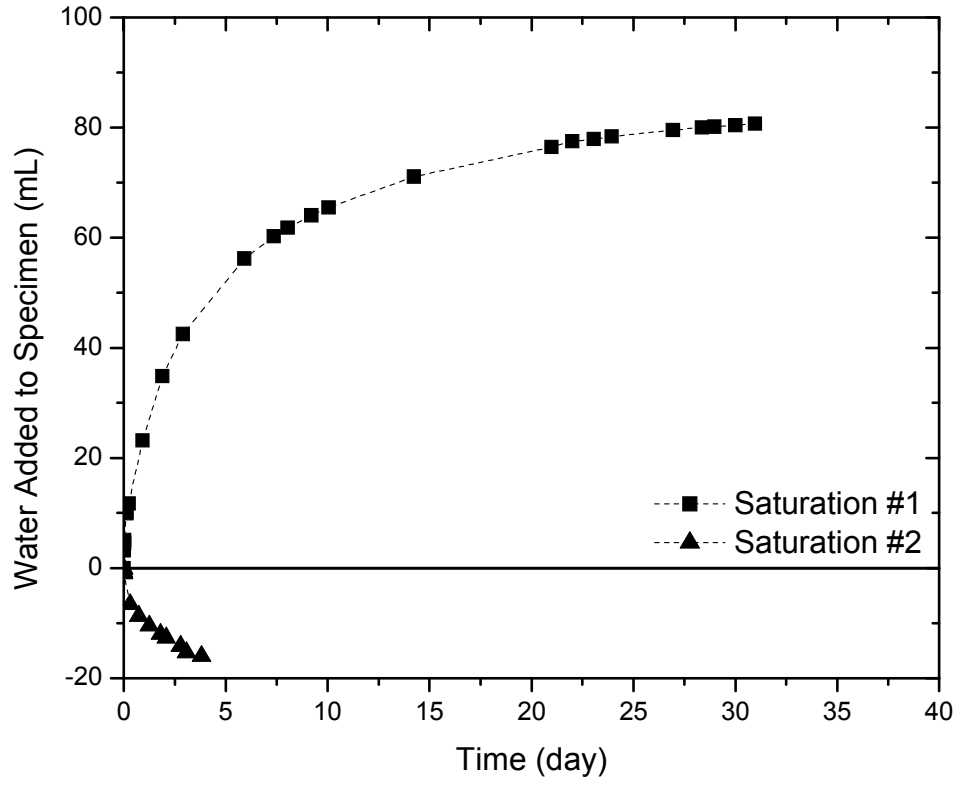


Figure 21: LBF Specimen JB-LB16: Saturation Phases

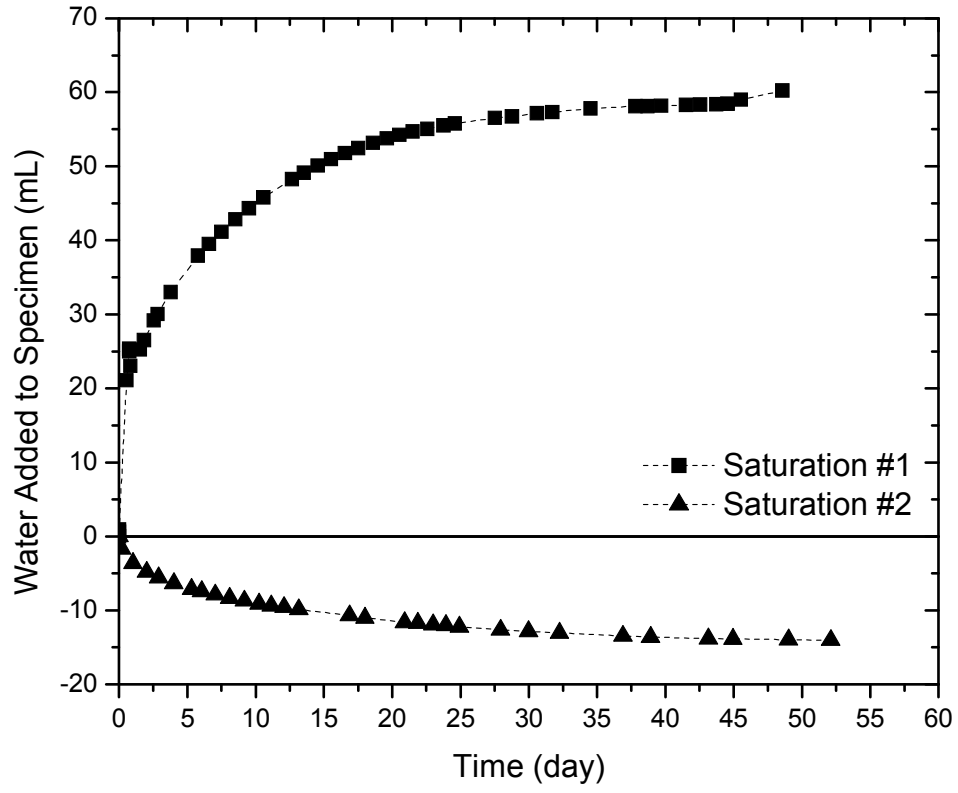


Figure 22: LBF Specimen JB-LB17: Saturation Phases

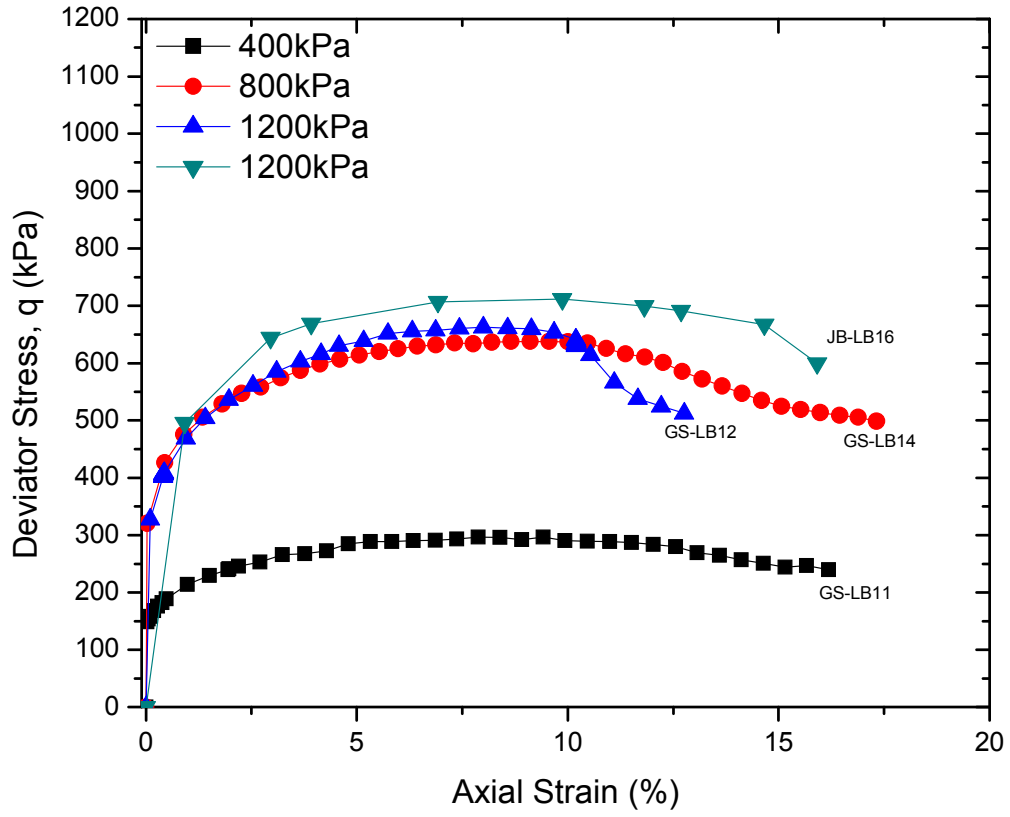


Figure 23: LBF Drained Shear Response: Deviator Stress Versus Axial Strain

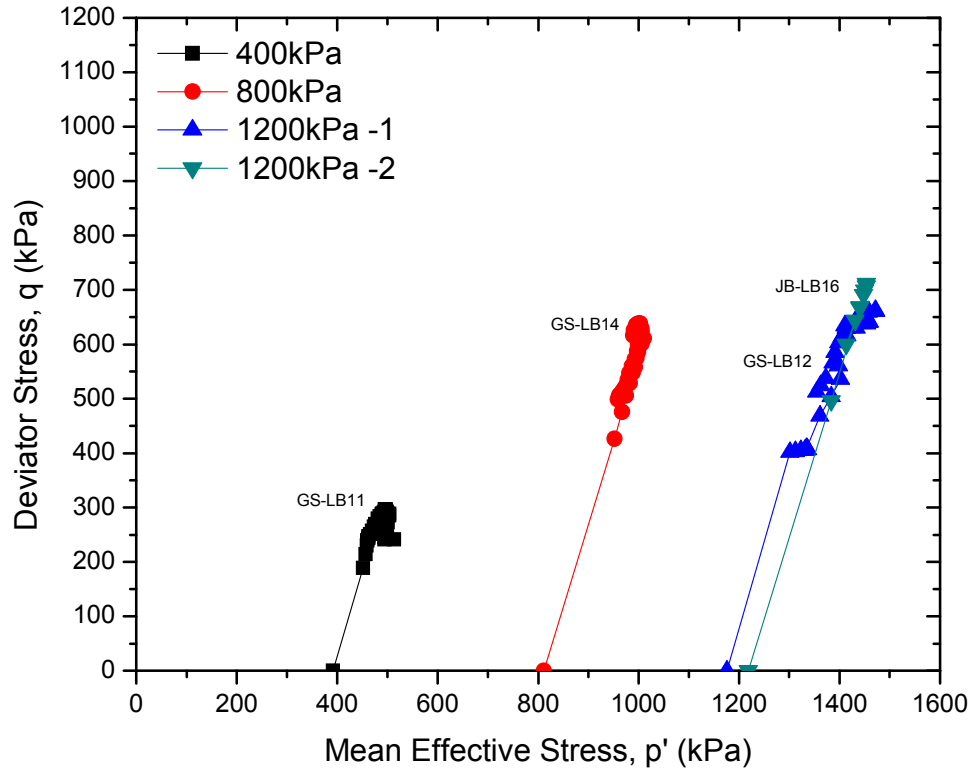


Figure 24: LBF Drained Shear Response: Deviator Stress Versus Mean Effective Stress

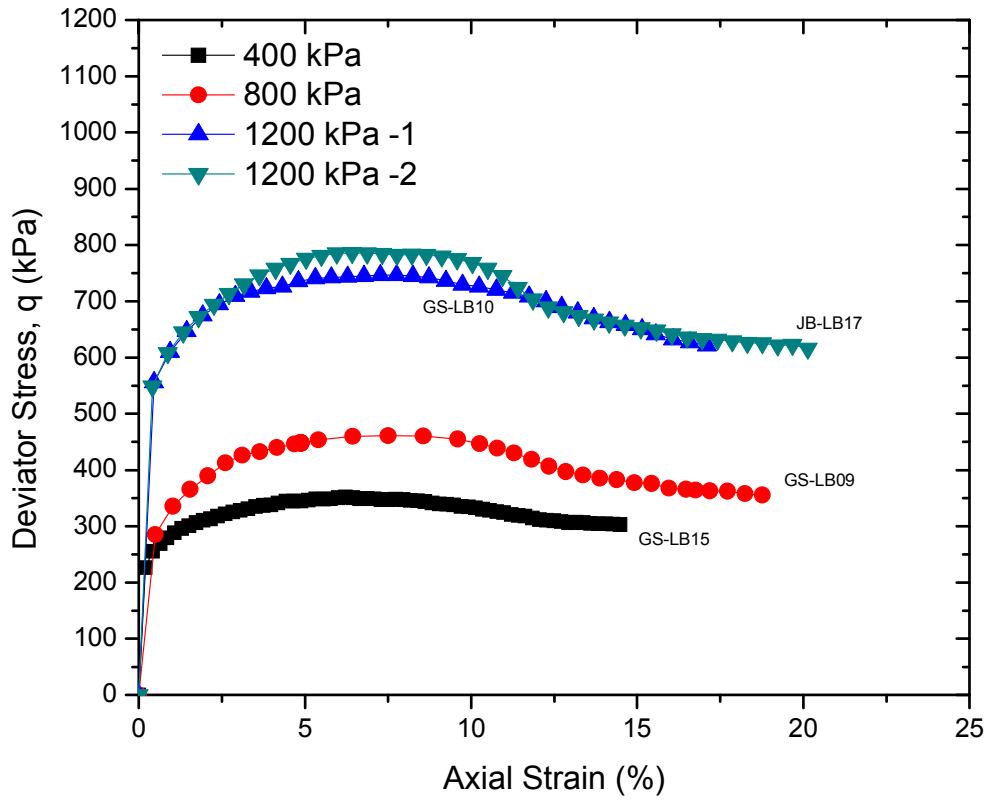


Figure 25: LBF Undrained Shear Response: Deviator Stress Versus Axial Strain

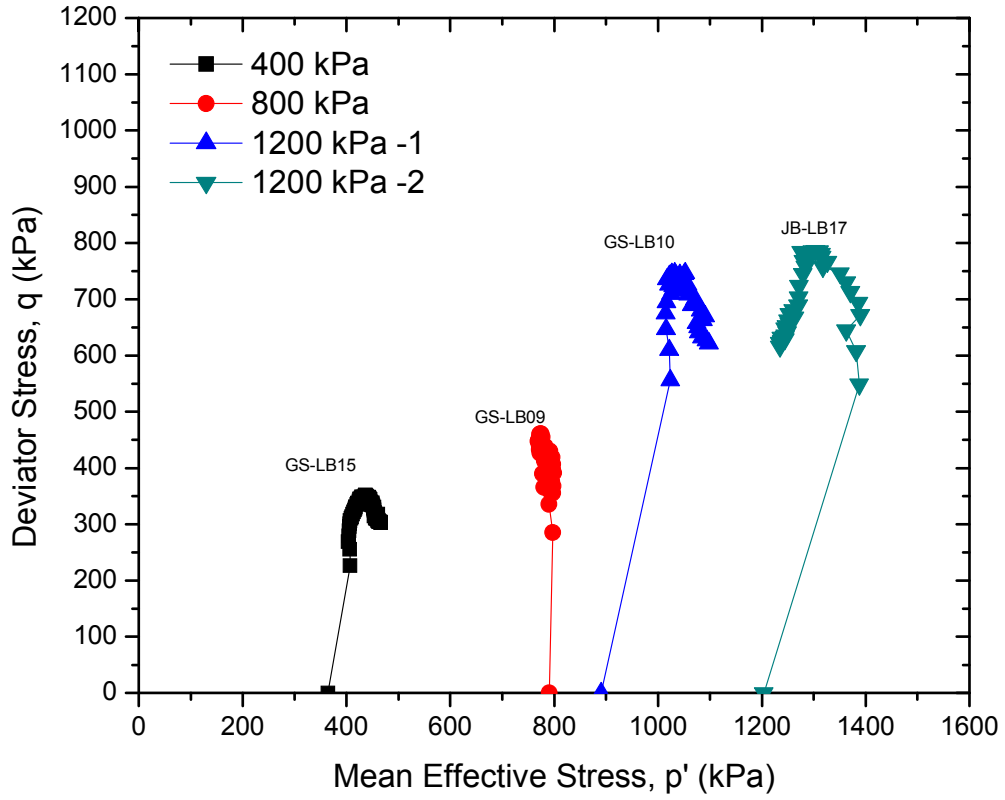


Figure 26: LBF Undrained Shear Response: Deviator Stress Versus Mean Effective Stress

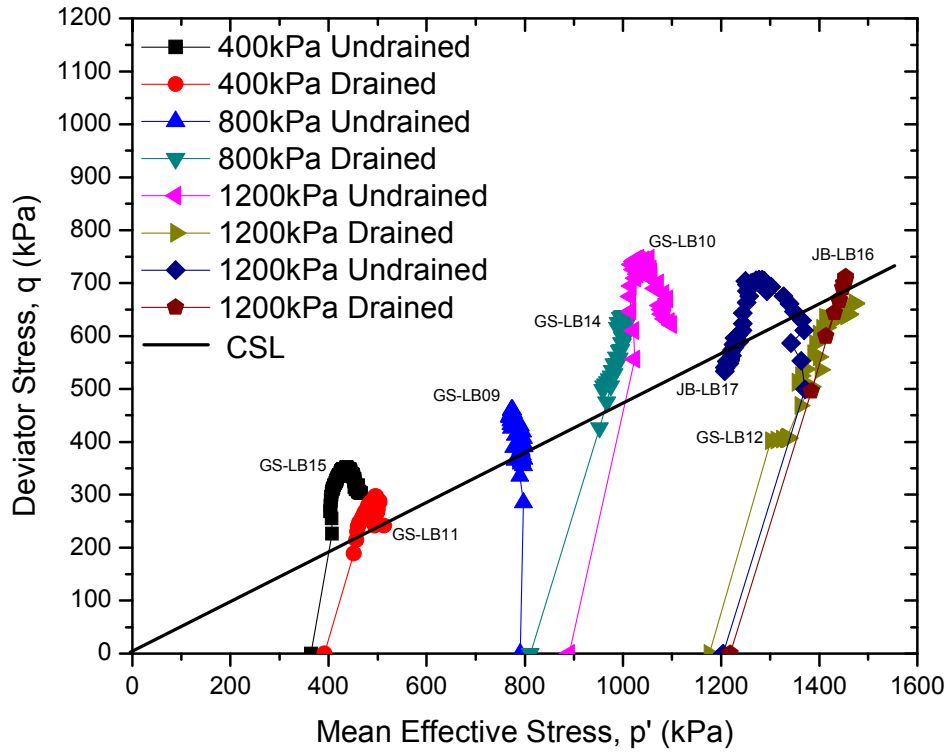


Figure 27: LBF Critical State Strength Envelope: Deviator Stress Versus Mean Effective Stress

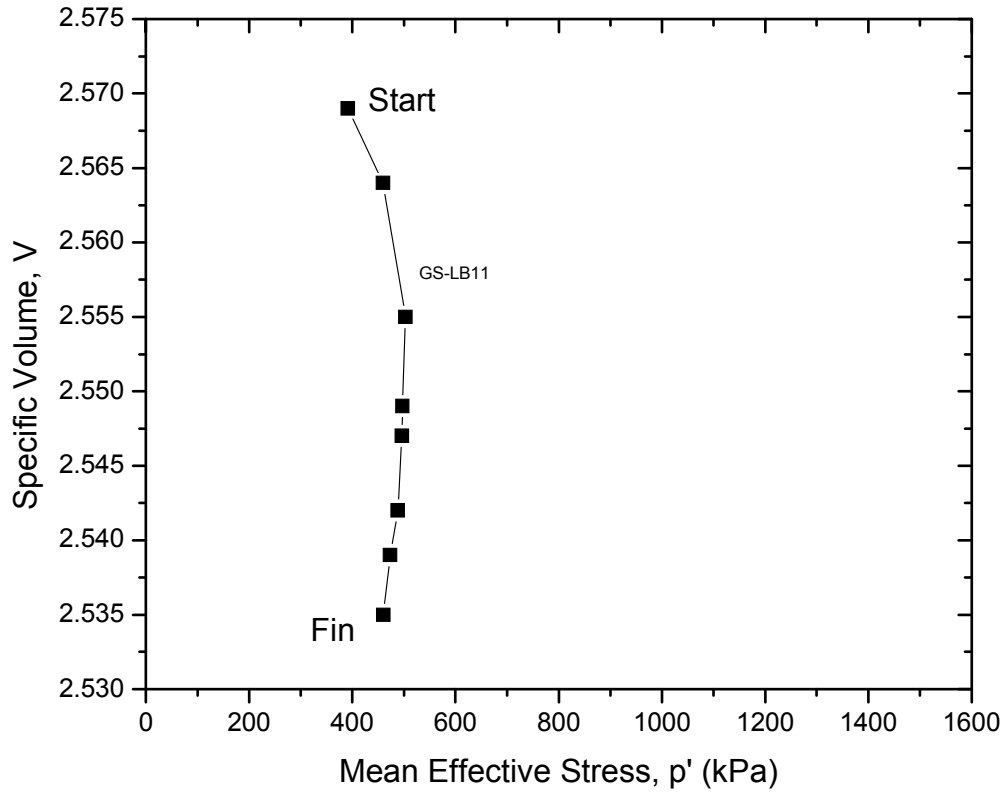


Figure 28: LBF Specimen GS-LB11 Volume Change During Drained Shearing at 400 kPa: Specific Volume Versus Mean Effective Stress

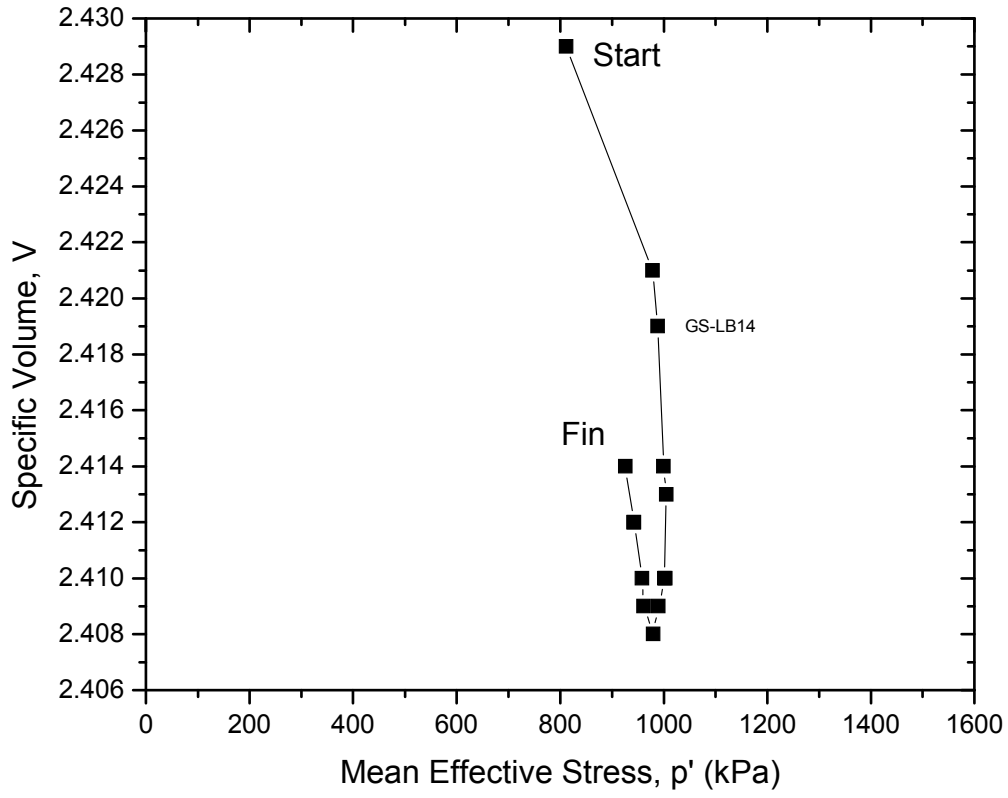


Figure 29: LBF Specimen GS-LB14 Volume Change During Drained Shearing at 800 kPa: Specific Volume Versus Mean Effective Stress

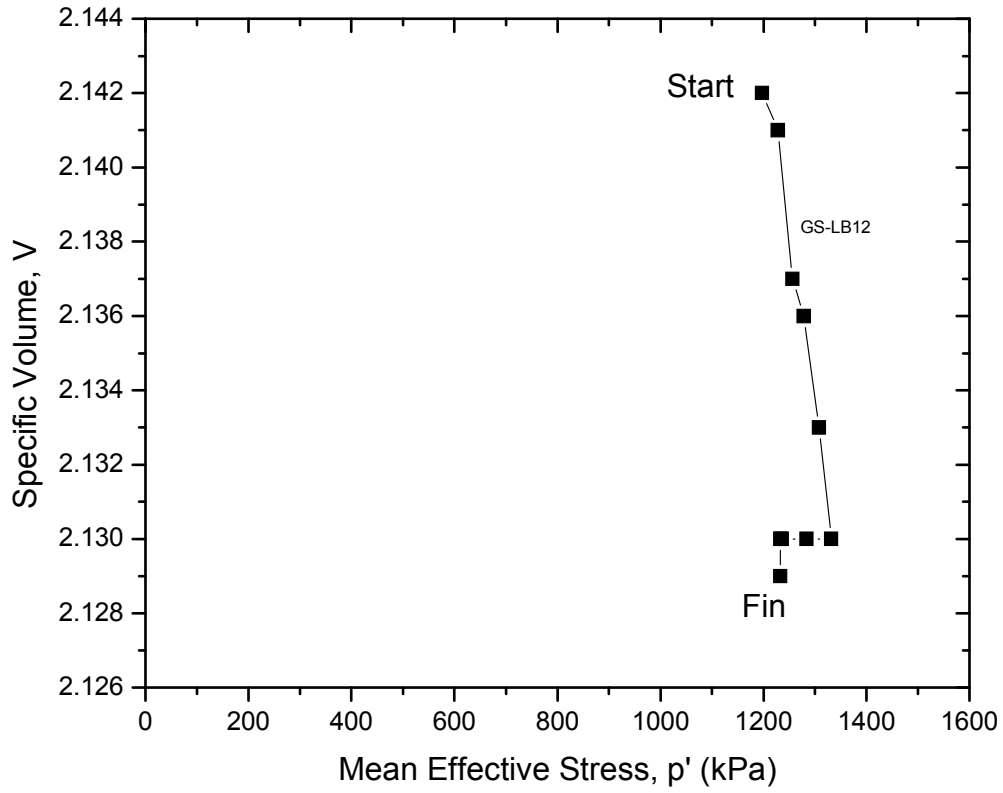


Figure 30: LBF Specimen GS-LB12 Volume Change During Drained Shearing at 1,200 kPa: Specific Volume Versus Mean Effective Stress

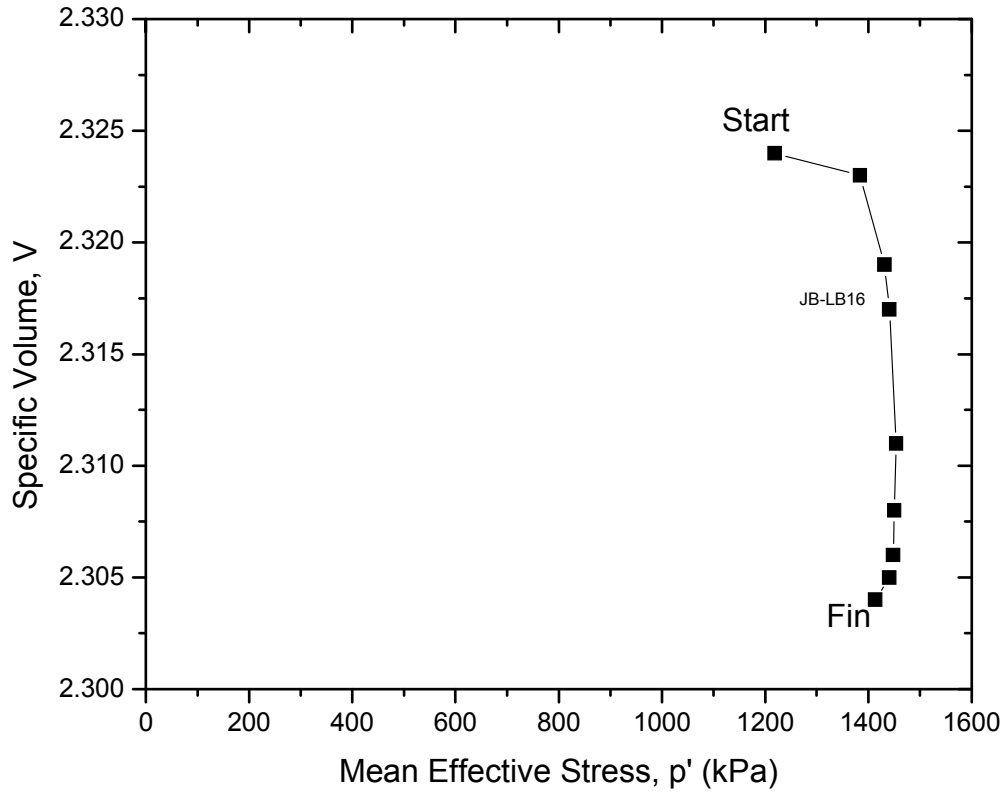


Figure 31: LBF Specimen JB-LB16 Volume Change During Drained Shearing at 1,200 kPa: Specific Volume Versus Mean Effective Stress

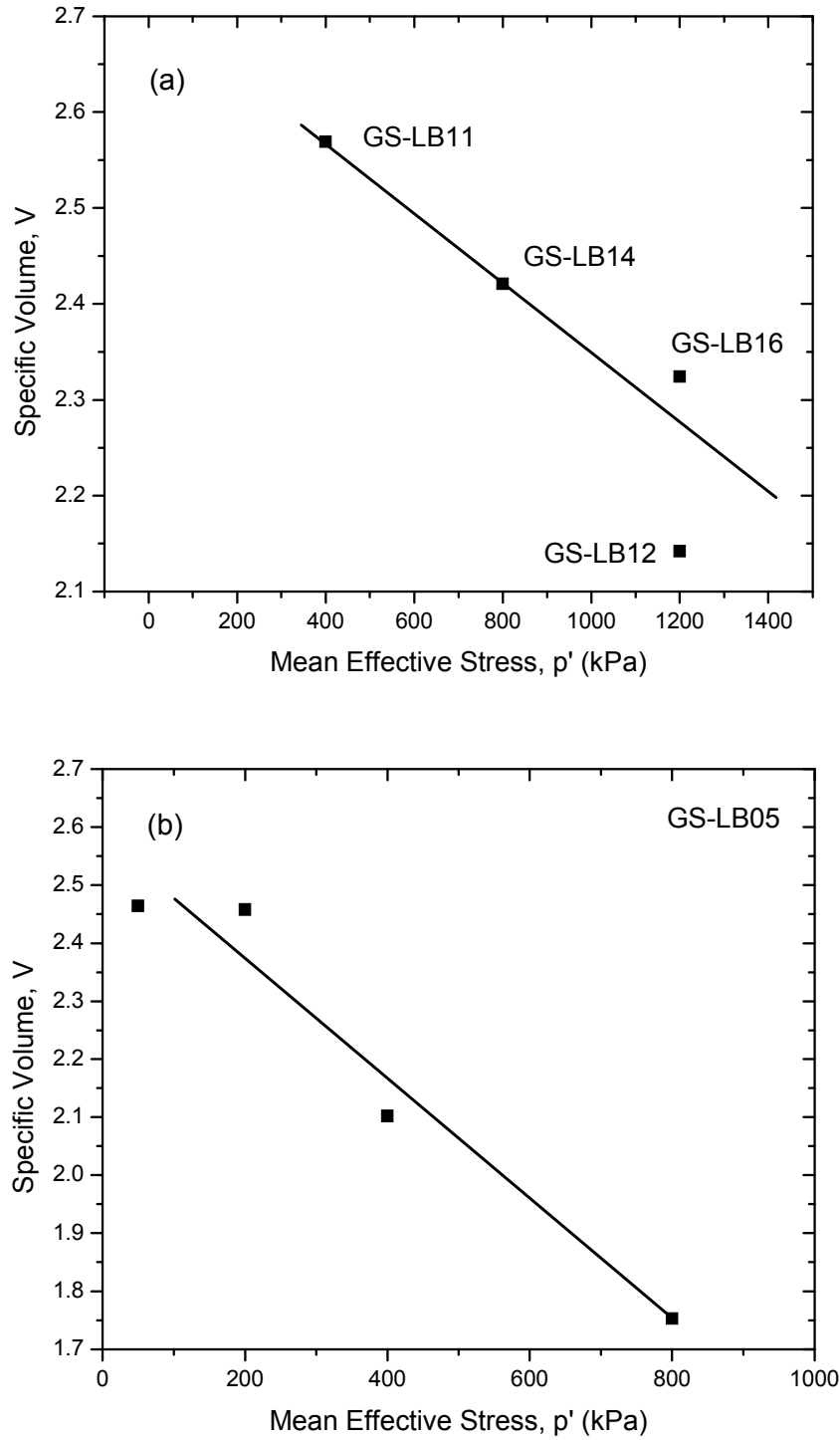


Figure 32: Isotropic Consolidation Data from Drained Tests on LBF Used for the Determination of the Bulk Modulus. The upper plot (a) was established by combining the end-of-consolidation data from the tests shown. The lower plot (b) was established from a single specimen (GS-LB05)

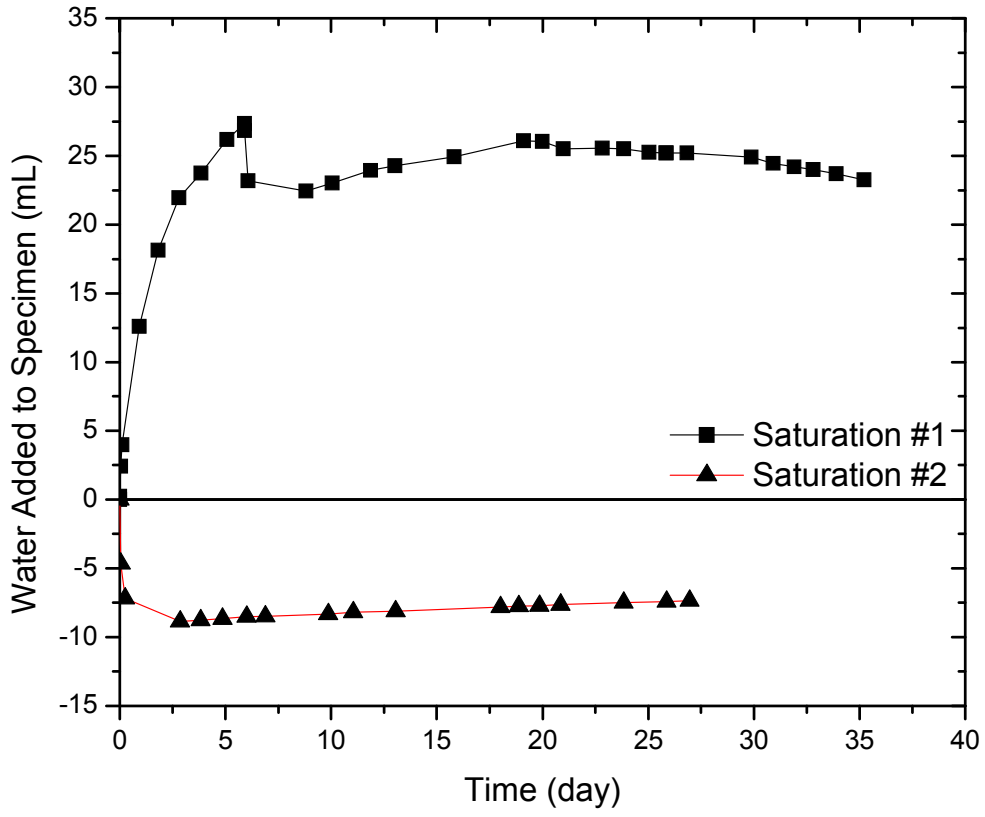


Figure 33: DBF Specimen GS-DBF13: Saturation Phases

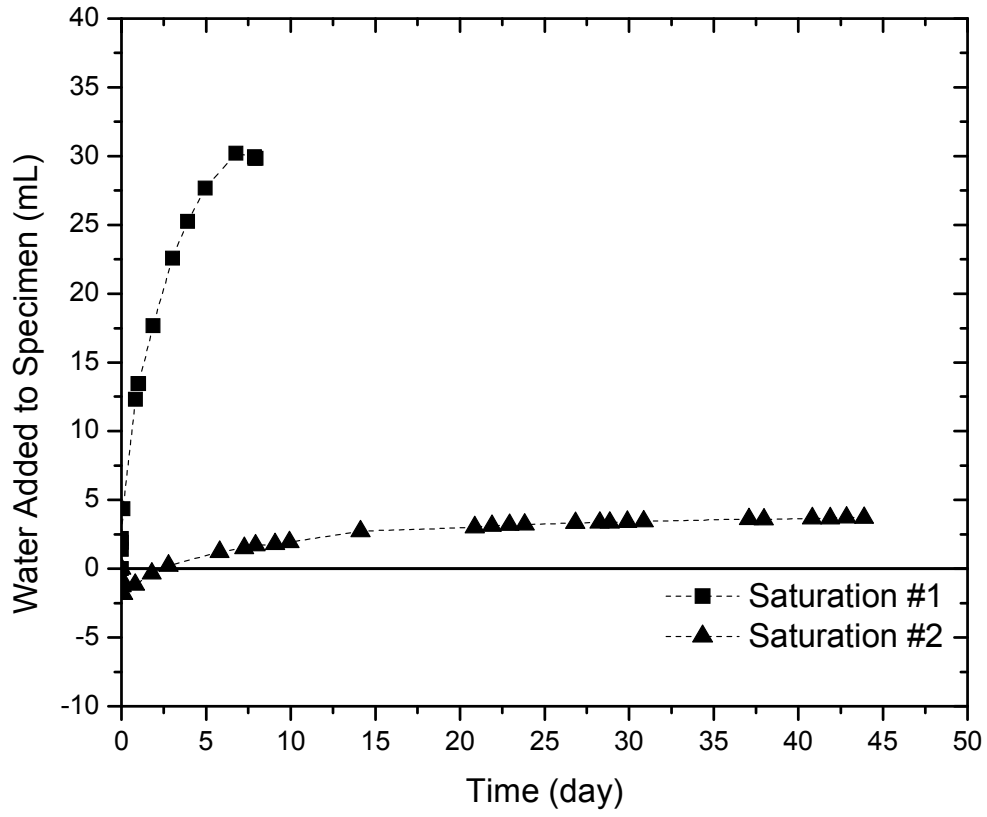


Figure 34: DBF Specimen JB-DBF14: Saturation Phases

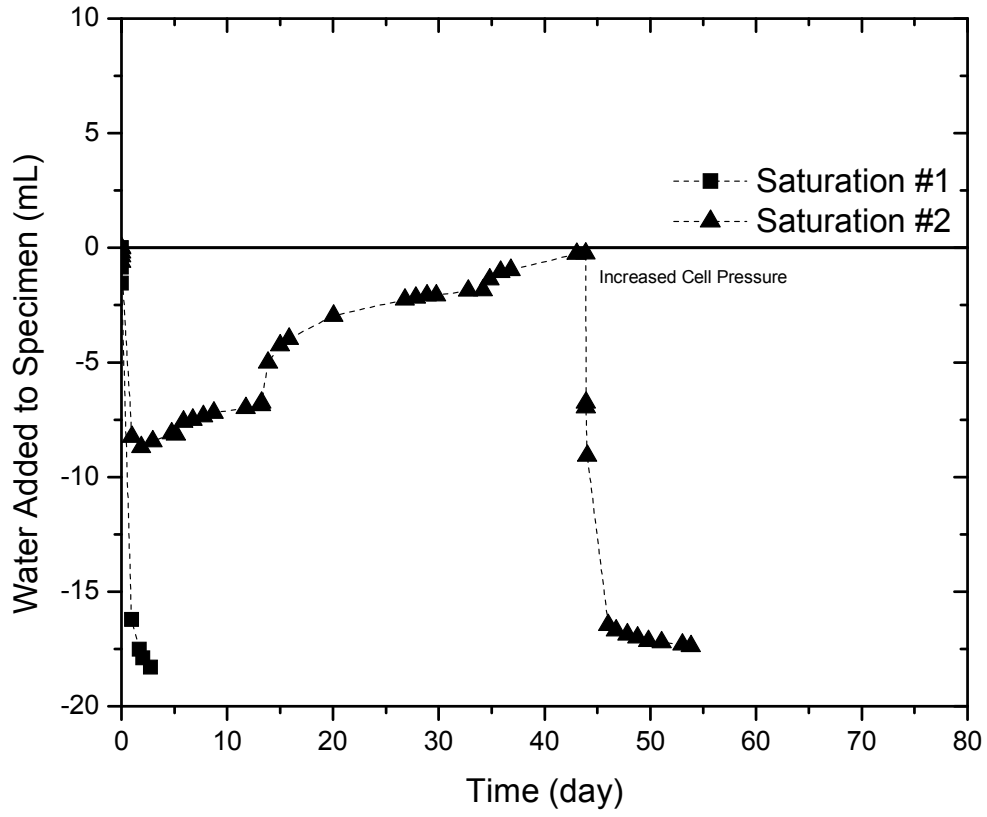


Figure 35: DBF Specimen GS-DBF15: Saturation Phases

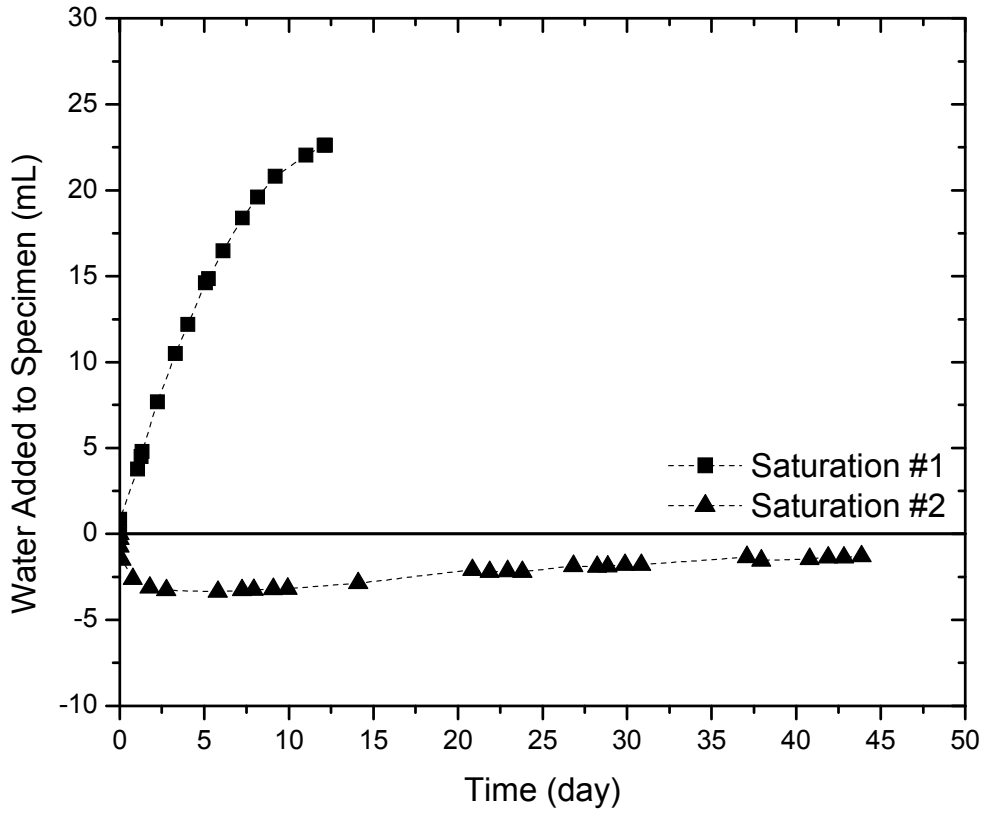


Figure 36: DBF Specimen JB-DBF16: Saturation Phases

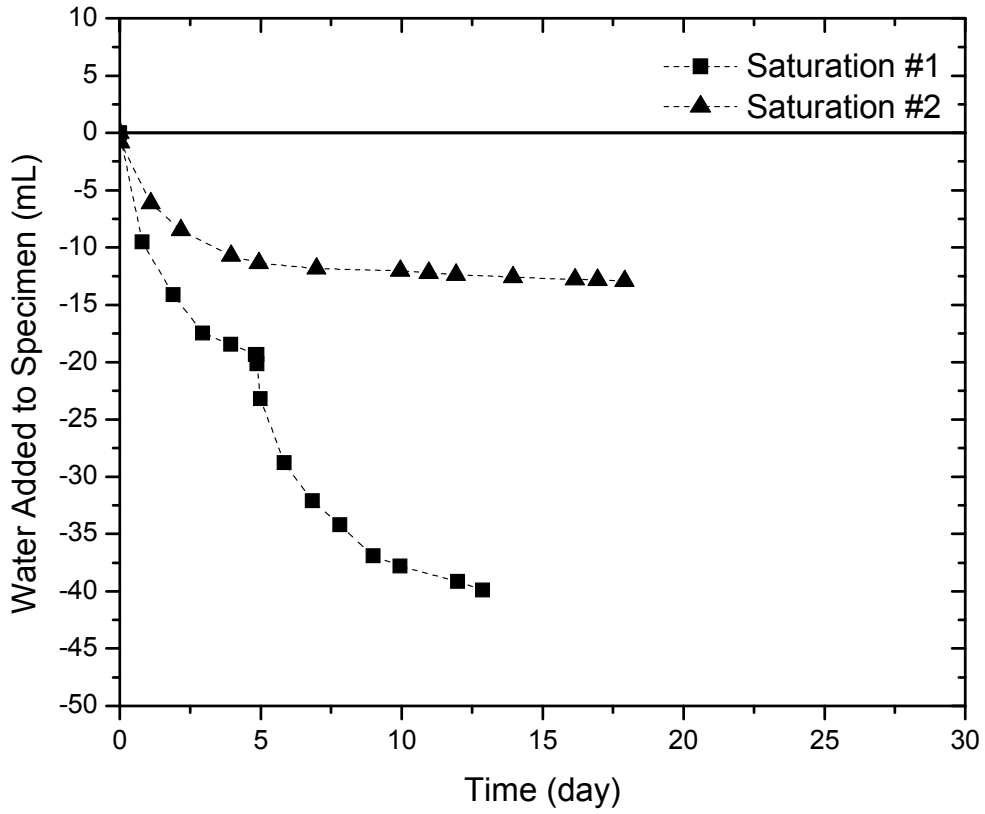


Figure 37: DBF Specimen GS-DBF17: Saturation Phases

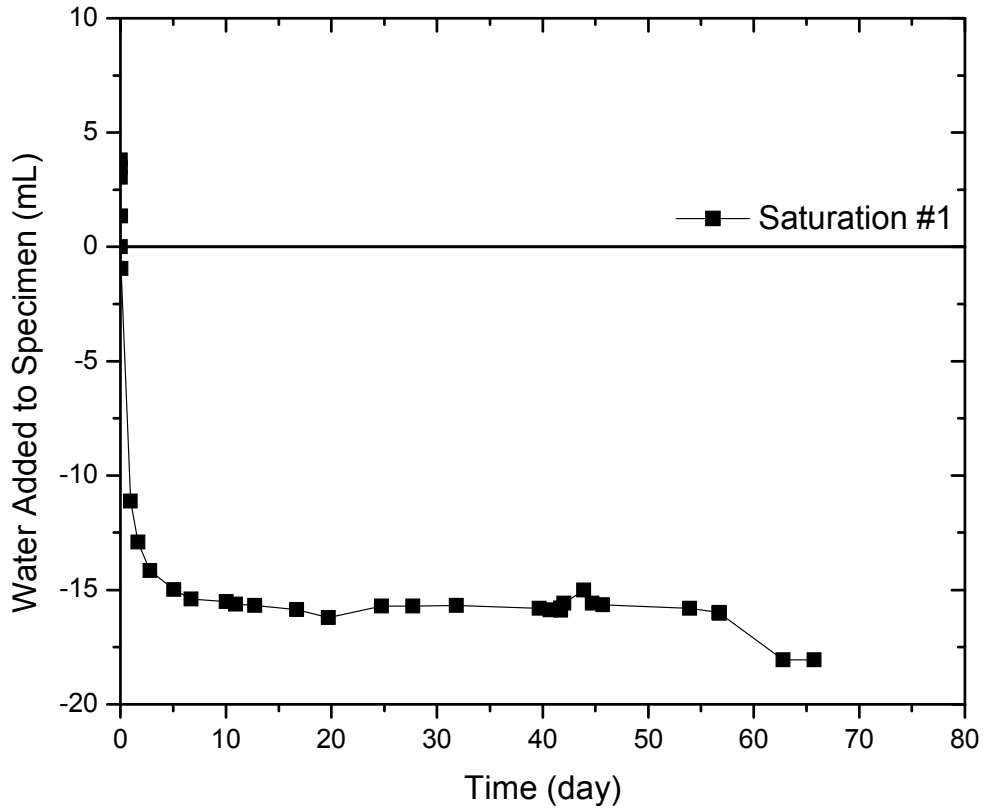


Figure 38: DBF Specimen GS-DBF18: Saturation Phases

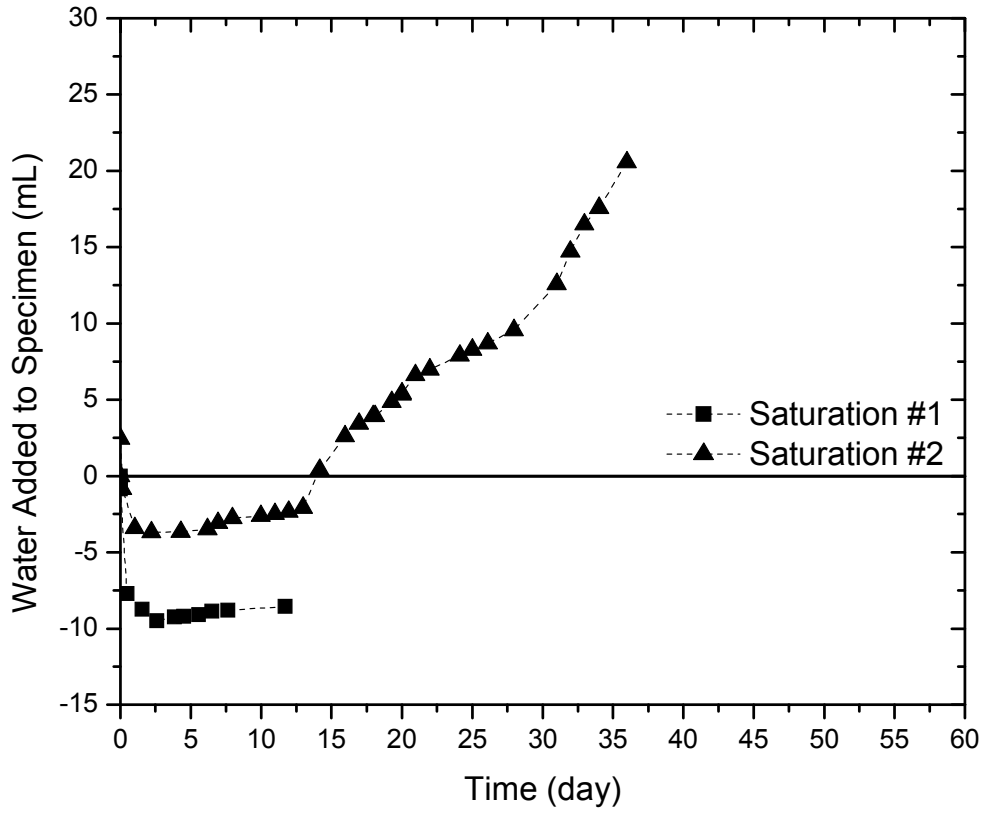


Figure 39: DBF Specimen GS-DBF19: Saturation Phases

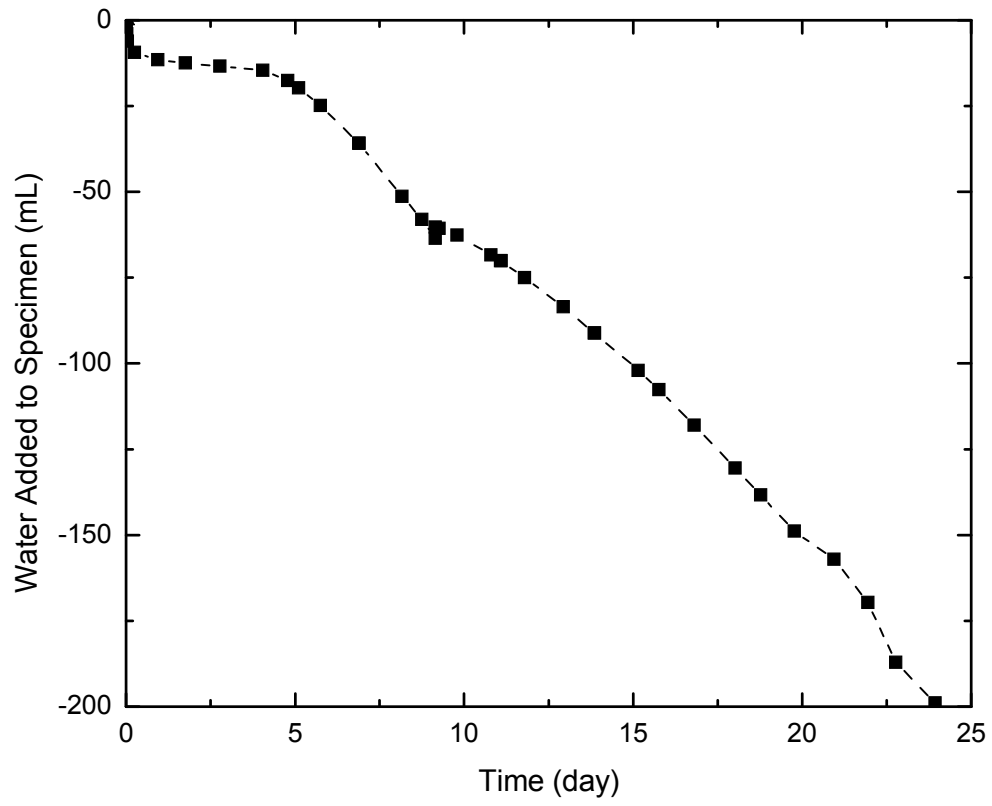


Figure 40: DBF Specimen GS-DBF20: Saturation Phases

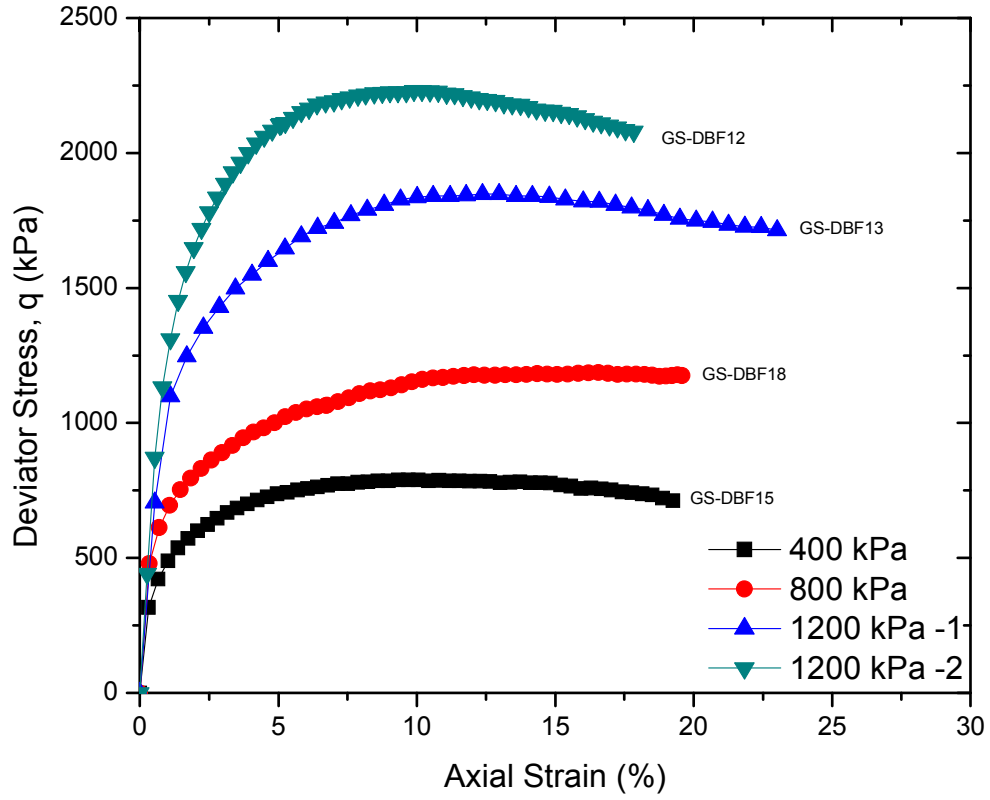


Figure 41: DBF Drained Shear Response: Deviator Stress Versus Axial Strain

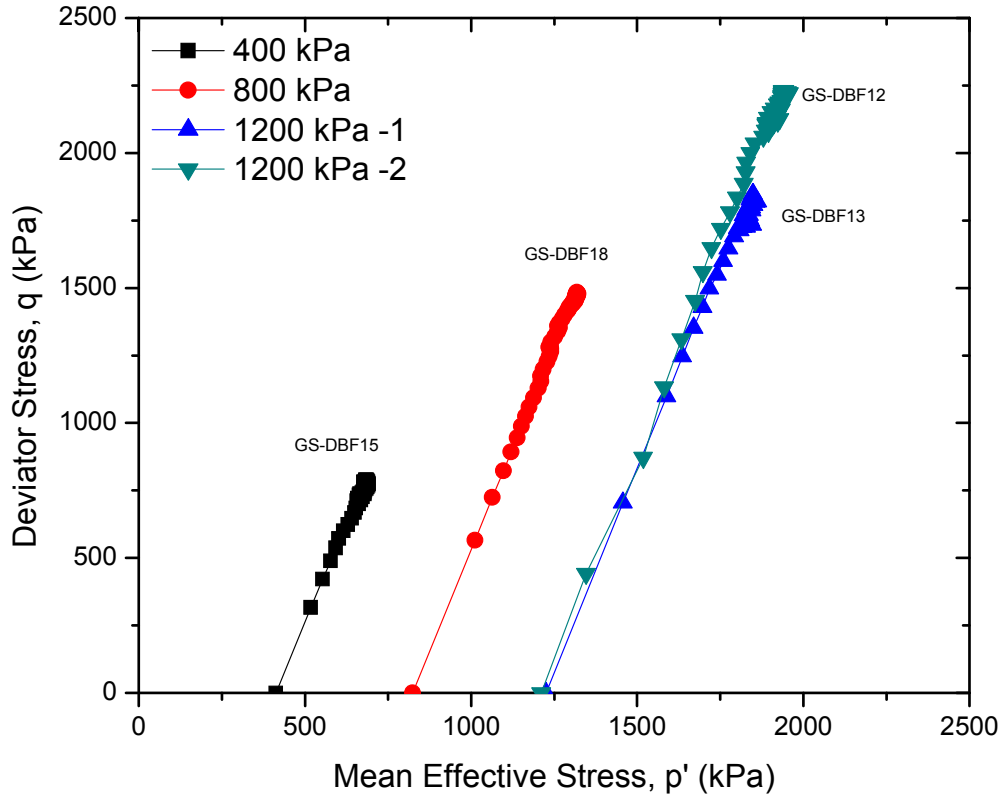


Figure 42: DBF Drained Shear Response: Deviator Stress Versus Mean Effective Stress

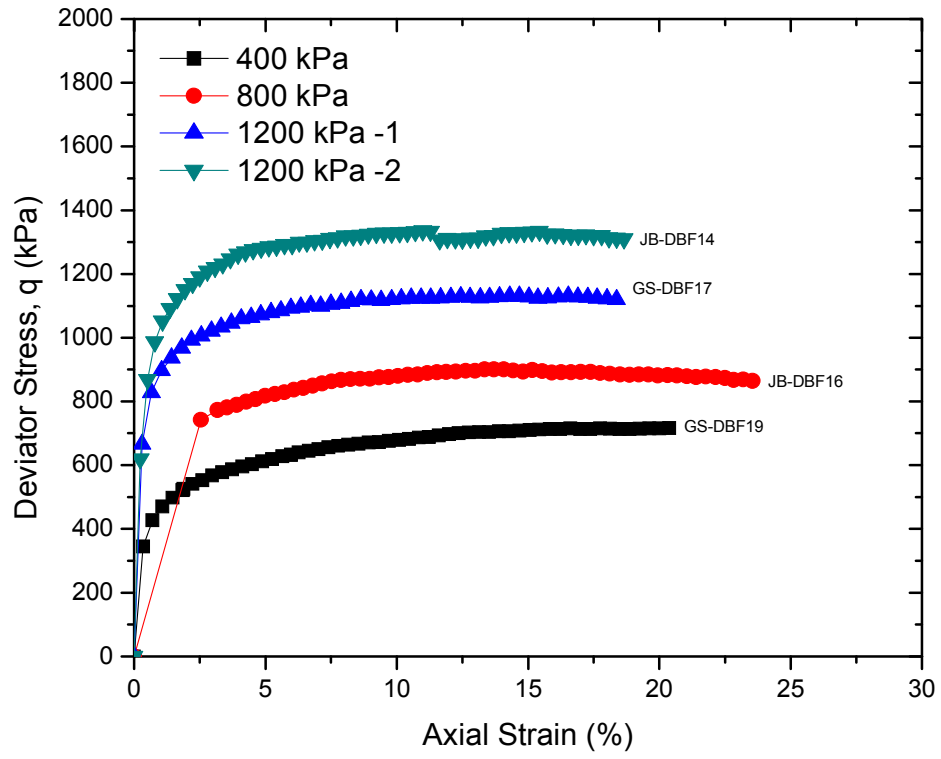


Figure 43: DBF Undrained Shear Response: Deviator Stress Versus Axial Strain

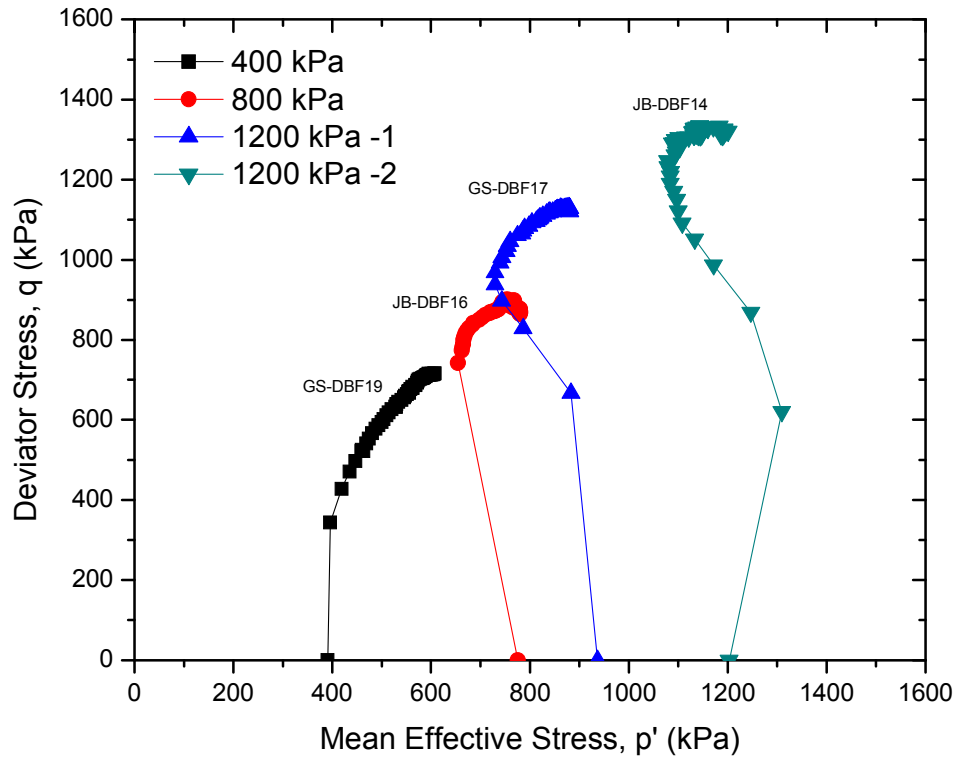


Figure 44: DBF Undrained Shear Response: Deviator Stress Versus Mean Effective Stress

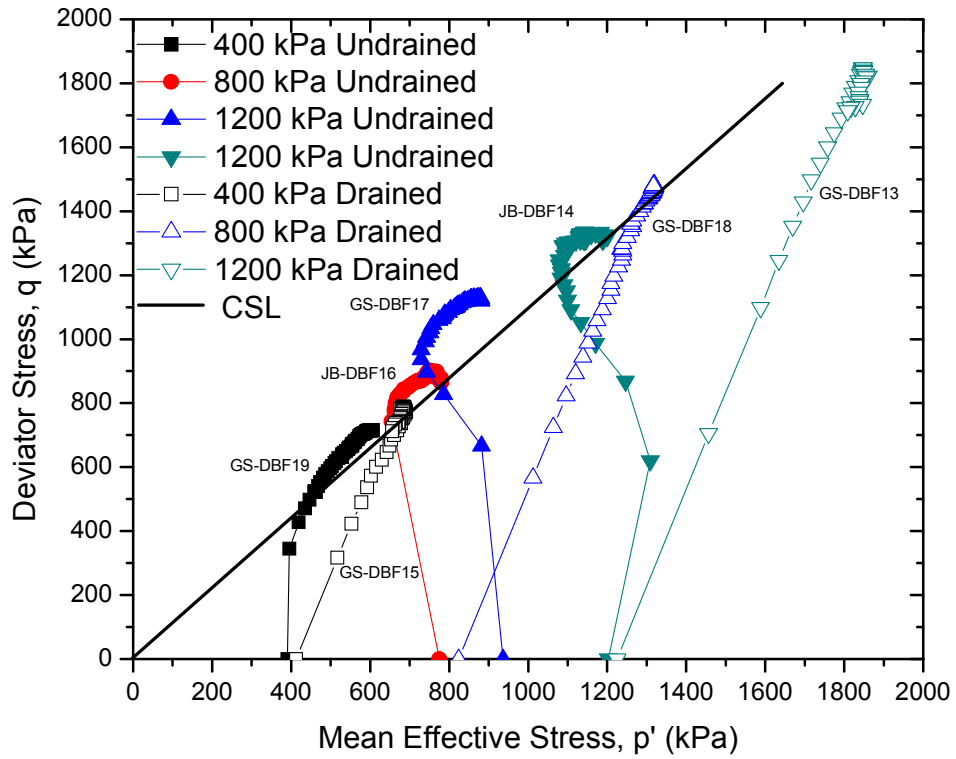


Figure 45: DBF Critical State Strength Envelope: Deviator Stress Versus Mean Effective Stress

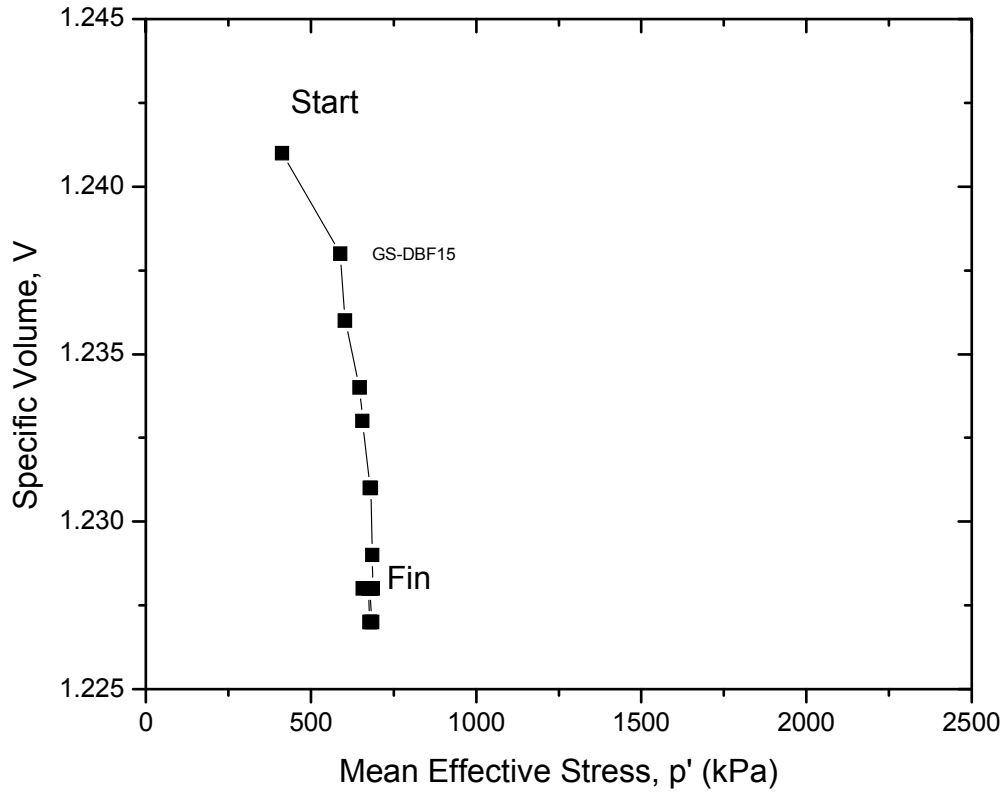


Figure 46: DBF Specimen GS-DBF15 Volume Change During Drained Shearing at 400 kPa: Specific Volume Versus Mean Effective Stress

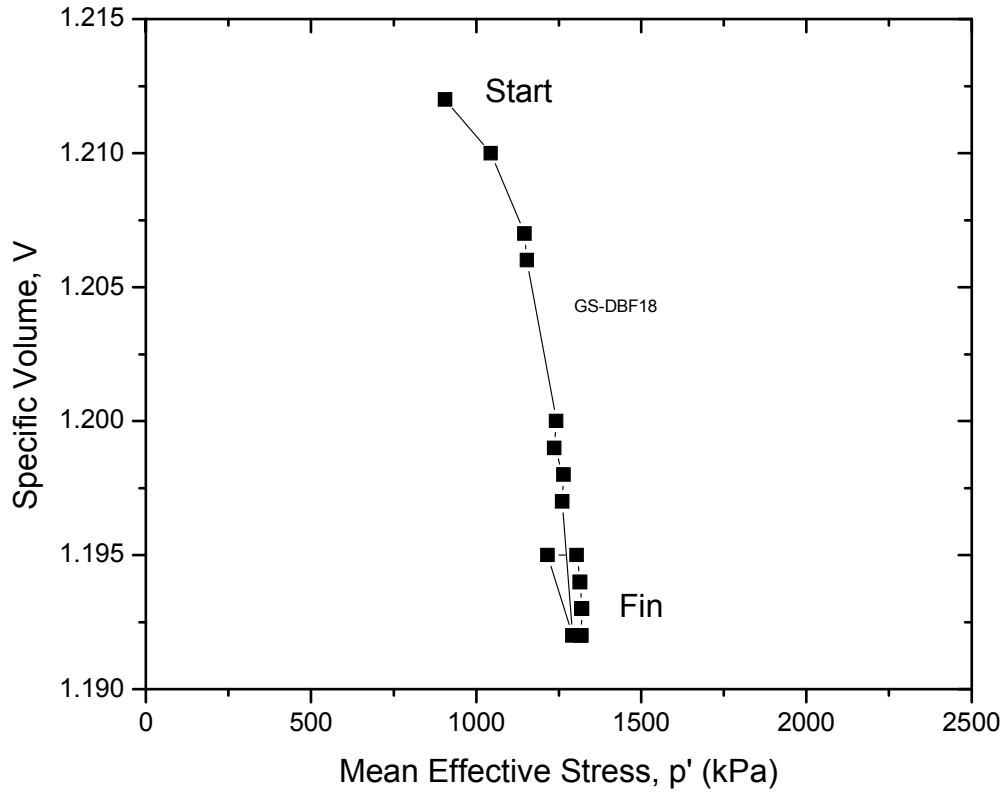


Figure 47: DBF Specimen GS-DBF18 Volume Change During Drained Shearing at 800 kPa: Specific Volume Versus Mean Effective Stress

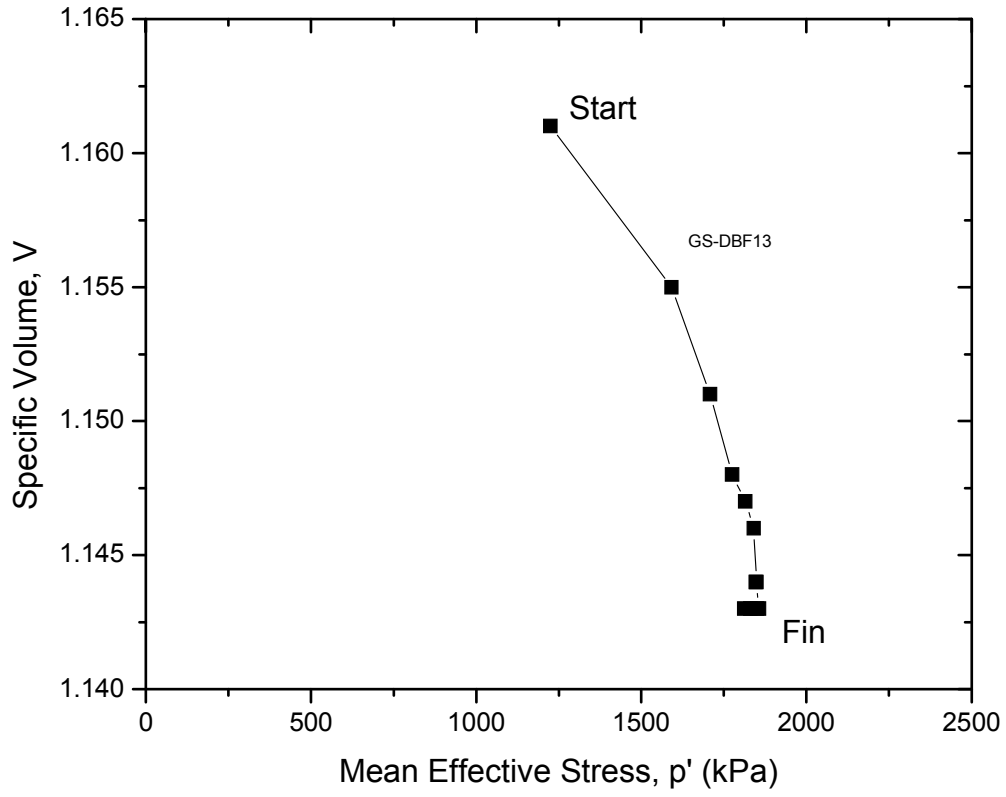


Figure 48: DBF Specimen GS-DBF13 Volume Change During Drained Shearing at 1,200 kPa: Specific Volume Versus Mean Effective Stress

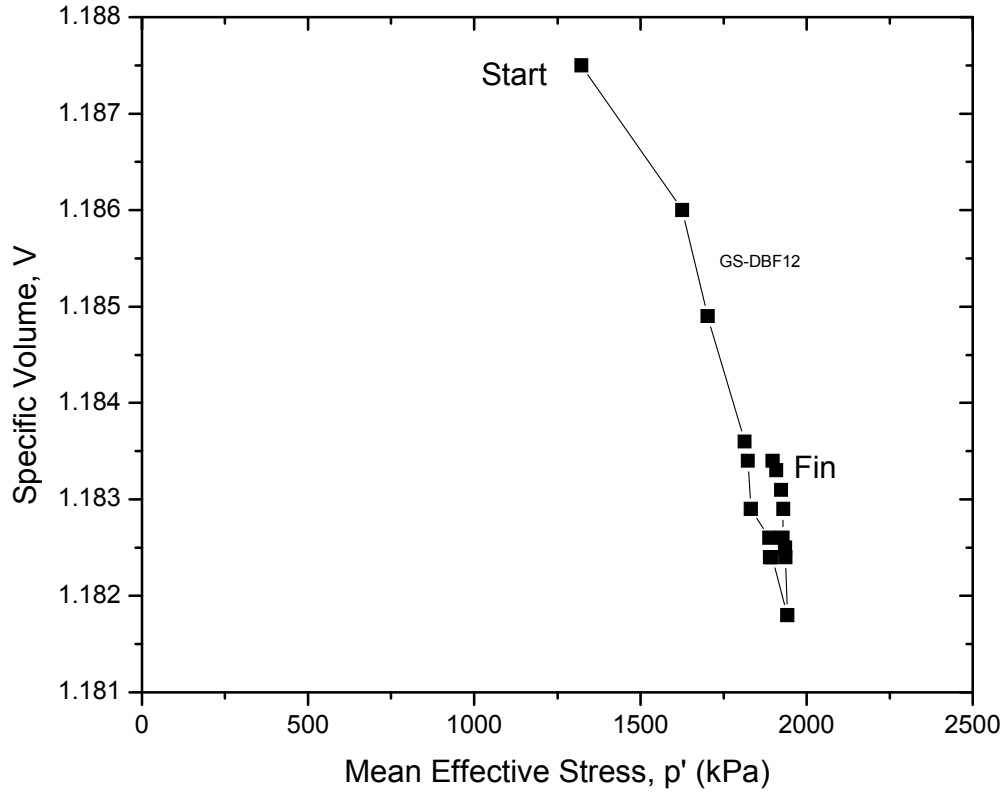


Figure 49: DBF Specimen GS-DBF12 Volume Change During Drained Shearing at 1,200 kPa: Specific Volume Versus Mean Effective Stress

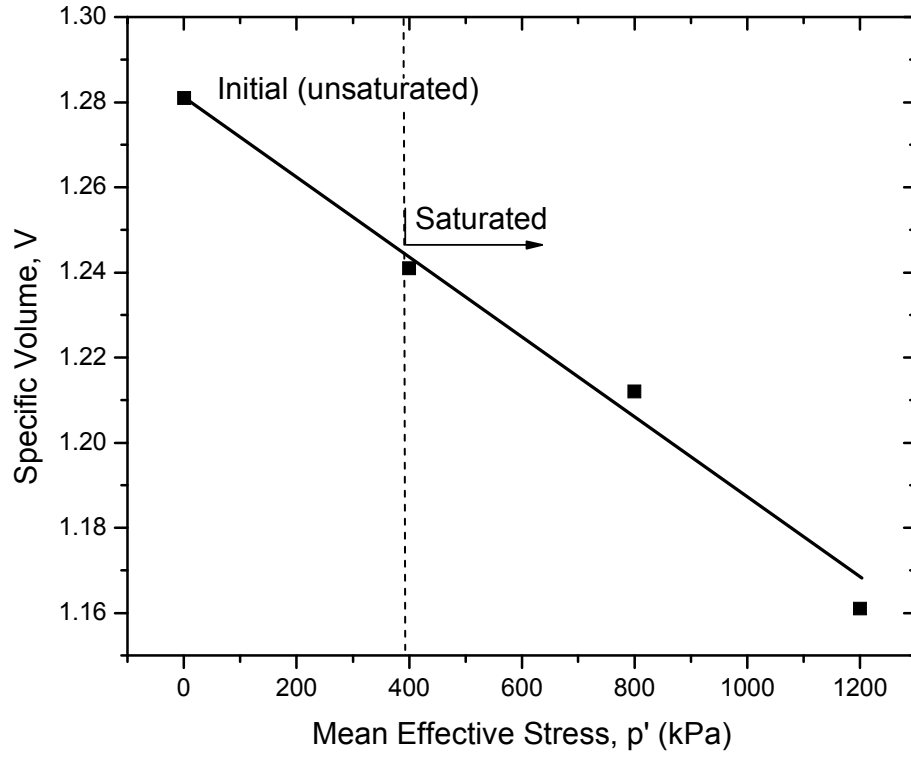


Figure 50: Isotropic Consolidation Data from Drained Tests on DBF Used for the Determination of the Bulk Modulus

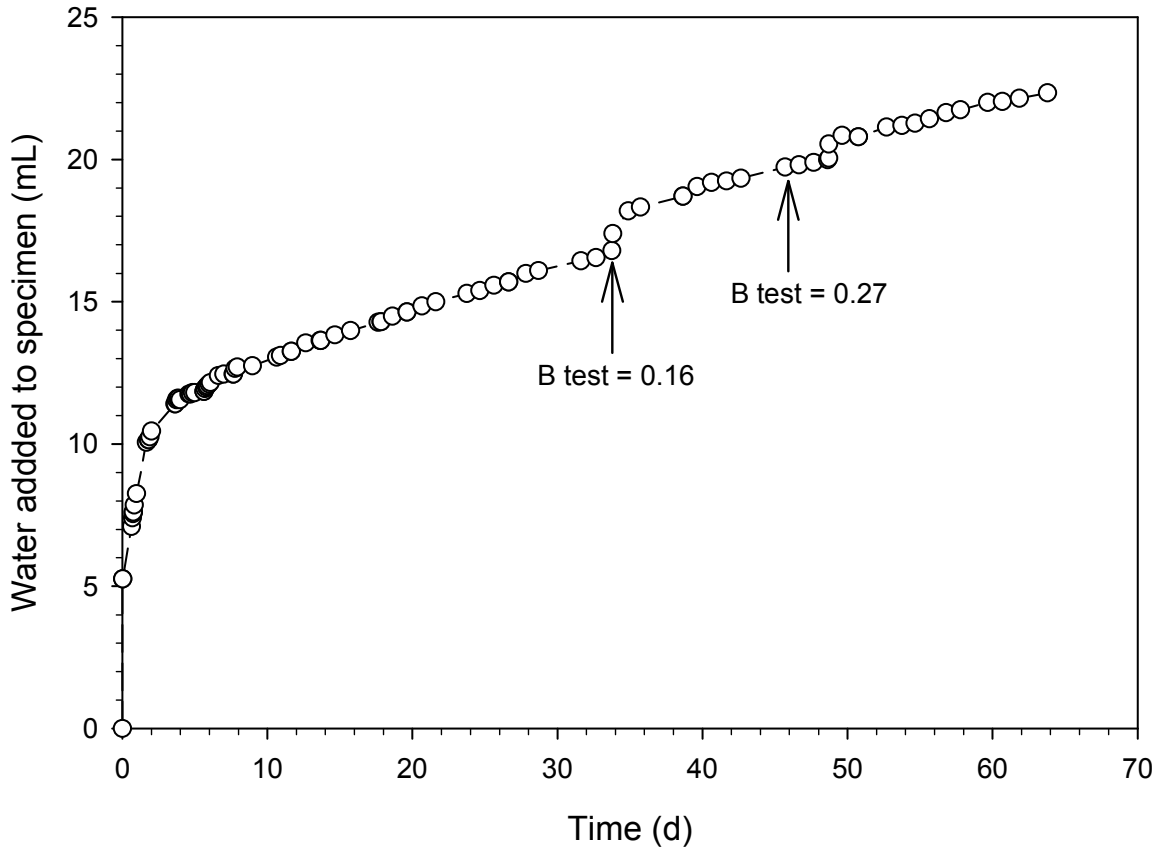


Figure 51: LBF Specimen LBF-1004: Saturation Phase (In progress)

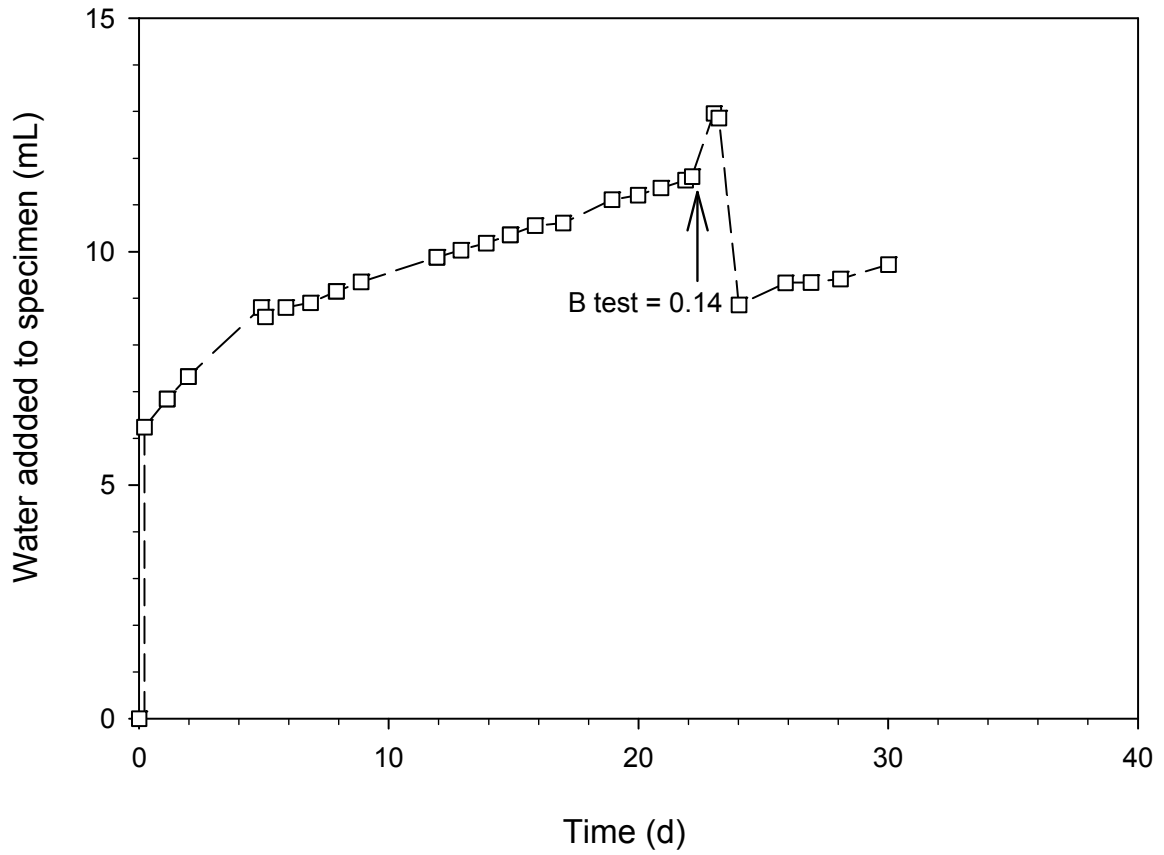


Figure 52: LBF Specimen LBF-1006: Saturation Phase (In progress)